Distribution-free precedence schemes with a generalized runs-rule for monitoring unknown location

J.C. Malela-Majika[a*], E.M Rapoo[a], A. Mukherjee[b] and M.A. Graham[c]

[a] *Department of Statistics, College of Science, Engineering and Technology, University of South Africa, PO Box 392 UNISA 0003, Pretoria, South Africa*

[b] *Department of Mathematics, Production, Operations and Decision Sciences Area, XLRI-Xavier School of Management, XLRI-Jamshedpur, India*

[c] *Department of Science, Mathematics & Technology Education, University of Pretoria, South Africa*

Abstract

Nonparametric statistical process monitoring schemes are robust alternatives to traditional parametric process monitoring schemes, especially when the assumption of normality is invalid or when we do not have enough information about the underlying process distribution. In this paper, we propose to improve the well-known precedence scheme using the 2-*of*-(*h*+1) runs-rules schemes (where $h > 1$). The performance of the proposed control schemes are thoroughly investigated using both Markov chain and simulations based approaches. We find that the proposed schemes outperform their competitors in many cases. A real-life example is given to illustrate the design and implementation of the proposed schemes.

Keywords: nonparametric scheme; precedence control scheme; generalized 2-*of*-(*h*+1) runs-rules schemes; Markov chain approach; simulations

1. Introduction

In these last two decades, many researchers have devoted their attention on nonparametric statistical process monitoring (NSPM) schemes. If the in-control (IC) run-length distribution and consequently, all the IC characteristics of a monitoring scheme are the same for every continuous probability distribution function (pdf), the scheme is referred to as "distribution-free" (or nonparametric). Distribution-free schemes are mostly recommended when the

[*] *Correspondence to: Jean-Claude Malela-Majika, Department of Statistics, College of Science, Engineering and Technology, University of South Africa, PO Box 392 UNISA 0003, Pretoria, South Africa*

Email address: malelm@unisa.ac.za

underlying distribution of the quality process is unknown or non-normal, for example, see Qiu (2014), Graham et al. (2017), Triantafyllou (2017), Mukherjee and Sen (2018), Patil and Shirke (2017) and Zombade and Ghute (2018). The plotting statistics of these schemes (or charts) are either the sign or sign-rank or Mann-Whitney or some order statistic of the observations. One of the most popular nonparametric schemes known as "the median scheme" was proposed by Janacek and Meikle (1997). The lower and upper control limits (LCL and UCL) of this scheme are given by two order statistics of the Phase I (or reference) sample X_1, X_2,…, X_m; and the plotting statistic is the median, M, of the Phase II (or test) sample Y_1, Y_2,…, Y_n. This scheme is considered to be the basic median scheme denoted by "1-*of*-1 scheme". The basic median scheme signals when the charting (or plotting) statistic plots on or outside of the control limits. Therefore, the basic scheme uses only one plotting statistic to decide whether the process is IC or out-of-control (OOC). Klein (2000) showed that the 1-*of*-1 (or basic) scheme is relatively insensitive to small shifts. To overcome this problem, many researchers suggested the addition of runs-rules; see for example, Derman and Ross (1997), Klein (2000), Chakraborti et al. (2009) and Tran (2017, 2018).

Traditional Shewhart-type schemes are usually more effective in detecting large and abrupt shifts in one or more process parameters. Nevertheless, they are often found to be less efficient for small to moderate shifts. Traditional Shewhart-type schemes are often integrated with supplementary runs-rules to improve their performance in detecting small and moderate shifts. A scheme is expected to give an OOC signal if one or more plotting statistics fall outside the control limits or when the plotted points do not exhibit a random pattern of behaviour. Balakrishnan and Koutras (2002) defined a run as an uninterrupted sequence of the same elements bordered at each end by other types of elements. Two types of runs exist in statistical process control and monitoring (SPCM), referred to as "run up" (when there is an increasing trend in the observed plotting statistics) and "run down" (when there is a decreasing trend in the observed plotting statistics). The runs are very important in assessing patterns on schemes. Western electric company (1956) and Nelson (1984) defined eight rules for detecting nonrandom patterns on schemes and later on, Trip and Does (2010) suggested four rules. For more details on the decision rules, readers are referred to Montgomery (2001). Different other types of rules (runs-rules) have been considered in the literature and they are mainly described as follows:

(i) the non-side-sensitive (NSS) *w*-*of*-(*w*+*v*) with $w > 1$ and $v \geq 0$ (by Derman and Ross (2010), hereafter DR) that signals when *w* out of *w*+*v* successive samples fall on or outside the control limits, no matter whether some (or all) of the *w* samples fall above the *UCL* and others (or all) fall below the *LCL* which are separated by at most *v* samples that fall between the control limits,

(ii) the side-sensitive *w*-*of*-(*w*+*v*) (by Klein (2000), hereafter KL) that signals when *w* samples out of *w*+*v* successive samples plot above (below) the *UCL* (*LCL*) which are separated by at most *v* samples that plot below (or above) the *UCL* (*LCL*), respectively.

Earlier in current decade, Human et al. (2010) and Kritzinger et al. (2014) investigated the performance of the nonparametric sign and signed-rank charts with supplementary runs-rules. The 2-*of*-2 precedence schemes were investigated by Chakraborti et al. (2009) and Malela-Majika et al. (2016a, 2016b). Shongwe and Graham (2016) explored the zero-state and steady-state performance of a variety of synthetic and runs-rules schemes. Rakitzis (2016) used two-sided schemes supplemented with runs-rules to monitor exponential data. Li et al. (2016) proposed a robust algorithm for an economic design of nonparametric schemes. More recently, several authors have investigated the properties of a variety of monitoring schemes supplemented with runs-rules, see for example, Maravelakis (2017), Rakitzis (2017), Patil and Shirke (2017), Chang et al. (2018) and Mehmood et al. (2018). The economic design of monitoring schemes supplemented with runs-rules was investigated by Lee and Khoo (2017) and Golbafian et al. (2017). Zombade and Ghute (2018) proposed a Shewhart-type nonparametric control chart for monitoring the process location. Tran (2017, 2018) proposed the median and *t* schemes with supplementary runs-rules for monitoring the process mean. The performances of these schemes are investigated using either exact formulae, simulations or the Markov chain approach. When using simulations to evaluate the performance of a scheme, an inerrant error of simulation occurs and this may considerably affect the results. This error can be minimized by increasing the number of simulations (or replications), which consequently increases the computational times required for computing the run-length characteristics. To fix this problem, researchers are recommended to use exact formulas or a Markov chain procedure, see for example, Li et al. (2014), Petcharat et al. (2015) and Dyer (2016).

In this paper, we use a Markov Chain approach to investigate the zero-state and steady-state performances of the two-sided generalized 2-*of*-(h+1) DR and KL Shewhart-type precedence schemes where h is a positive integer ($h > 0$). The investigation is carried in terms of their IC and OOC unconditional average run length (*UARL*). We also use the extra quadratic loss function (EQL), as in Shongwe and Graham (2016), to investigate the overall zero-state and steady-state performances of the proposed schemes for different shift ranges. Extensive simulations (with 100000 replications) are also used to check the accuracy of the results. The investigation of the performance of the improved 2-*of*-(h+1) DR and KL schemes (i.e. the 1-*of*-1 or 2-*of*-(h+1) DR and KL Shewhart-type precedence schemes) will be discussed in a separate article. Note that Chakraborti et al. (2009) proposed a class of precedence charts based on the 2-*of*-2 scheme which is a particular case of the proposed generalized 2-*of*-(h+1) DR and KL precedence charts when $h = 1$ and explored the zero-state performance only.

Therefore, in this paper, we first investigate the IC and OOC performances of the 2-*of*-(h+1) for $h \geq 1$ (as Chakraborti, Eryilmaz, and Human (2009) and Malela-Majika, Chakraborti, and Graham (2016) did for $h = 1$ (only)). Secondly, we use a Markov chain approach slightly different from that in Chakraborti, Eryilmaz, and Human (2009). While Chakraborti, Eryilmaz, and Human (2009) studied the zero-state performance only, here, we study both the zero- and steady-state modes. Finally, the overall performance metric, i.e. zero- and steady-state average *EQL* (*AEQL*) values are computed to supplement the specific shift metric i.e. zero- and steady-state average run-length (*ARL*) values.

The remainder of this paper is organized as follows: in Section 2, firstly the 1-*of*-1 (i.e. basic) median precedence scheme is introduced, and, secondly, the general form of the transition probability matrices (TPMs) of the generalized 2-*of*-(h+1) DR and KL schemes are given. In Section 3, the performance measures and the expressions of the zero-state and steady-state *ARL* for both DR and KL schemes, are developed. Section 4 provides the design and implementation of the proposed charts and discusses the IC and OOC zero-state and steady-state performances of the 2-*of*-(h+1) DR and KL Shewhart-type precedence schemes. In Section 5, the effect of the Phase I sample size on the Phase II performance, of the proposed schemes, are investigated using extensive simulations. A real-life application of the proposed schemes is given in Section 6. Section 7 gives a concluding summary and some recommendations.

2. Shewhart-type precedence scheme with supplementary runs-rules

2.1 1-of-1 precedence scheme

Let $X = \{X_1, X_2, \ldots, X_m\}$ be a reference sample of size m available from an IC process with an unknown continuous cdf $F(x)$. Let Y_j^h (with $j = 1, 2, \ldots, n$ and $h = 1, 2, \ldots$) denote the h^{th} test sample of size n_h, $n_h = n\ \forall h$, since we are assuming that the Phase II samples are all of the same size. For instance, $Y_j^1 = \{Y_1, Y_2, \ldots, Y_n\}$ is the first test sample of size n. Let $G^h(y)$ denote the cdf of the distribution of the h^{th} Phase II sample and let $G^h(y) = G(y)\ \forall h$, since the Phase II samples are all assumed to be identically distributed. Let assume that the location model is given by $G(t) = F(t - \delta)$, for all t, where δ is the location difference (or shift in the location parameter). The process is IC in Phase II when $G = F$ which happens when $\delta = 0$.

The precedence scheme is a general class of nonparametric schemes that uses the j^{th} order statistic in the Phase II sample $Y_{(j:n)}$ (such as the minimum, lower quartile, median, upper quartile and maximum) as the charting statistic. In the case of the two-sided Shewhart-type precedence scheme, the charting statistic $Y_{(j:n)}$ is compared to the LCL and UCL which are given by the a^{th} and b^{th} order statistics of the Phase I sample, denoted $X_{(a:m)}$ and $X_{(b:m)}$ respectively, where $1 \leq a < b \leq m$ (see Figure 1). When j = 1, the corresponding precedence scheme is referred to as the minimum precedence scheme. However, when j = n, the precedence scheme is referred to as the maximum precedence scheme. When n is odd, say, $n = 2r + 1$, then $j = r + 1$ corresponds to the unique test sample median and the corresponding precedence scheme is called median precedence scheme. In the current paper, we consider the median precedence scheme and, only for brevity and simplicity throughout the paper, we refer to it as the precedence scheme, omitting the word median.

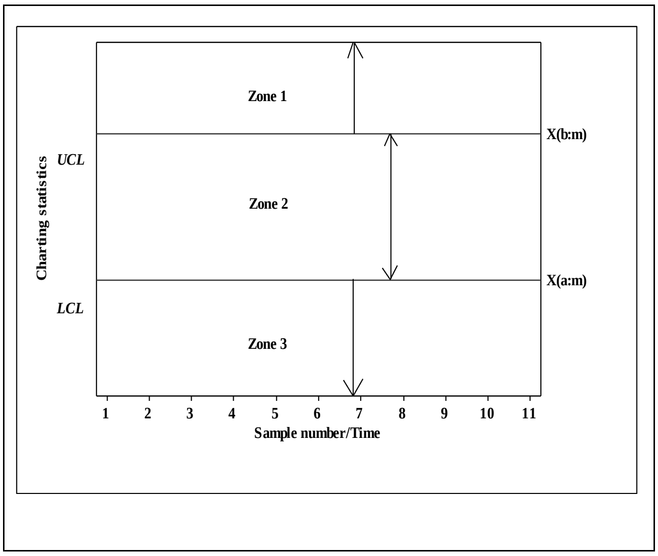

Figure 1. Different zones of the proposed control schemes

For the precedence scheme with known process parameters (that is, under Case K), we determined a as well as b and, consequently, the control limits, by setting the false alarm rate (*FAR*) to a desirable small value, say 0.0027 or 0.0020. The process is said to be OOC at the i^{th} sampling time if the charting statistic $Y_{(j:n)} \geq UCL$ or $Y_{(j:n)} \leq LCL$.

In Phase II, the random variable Y follows a beta distribution with parameters j and $n-j+1$ (see for example, Mukherjee, Graham, and Chakraborti 2013). Therefore, the conditional probabilities that the charting statistic plots in Zones 1, 2 and 3 (see Figure 1) are given by $p_0 = P\left(Y_{(j:n)} \in \theta\right)$ where $\theta \in \{1,2,3\}$:

$$p_1 = P\left(Y_{(j:n)} \geq X_{(b:m)} \middle| X_{(b:m)} = x_{(b:m)}\right) = I\left(GF^{-1}\left(U_{(b:m)}\right), j, n-j+1\right), \quad (1)$$

$$\begin{aligned} p_2 &= P\left(X_{(a:m)} \leq Y_{(j:n)} \leq X_{(b:m)} \middle| X_{(a:m)} = x_{(a:m)}, X_{(b:m)} = x_{(b:m)}\right) \\ &= I\left(GF^{-1}\left(U_{(b:m)}\right), j, n-j+1\right) - I\left(GF^{-1}\left(U_{(a:m)}\right), j, n-j+1\right) \end{aligned} \quad (2)$$

and

$$p_3 = P\left(Y_{(j:n)} \leq X_{(a:m)} \middle| X_{(a:m)} = X_{(a:m)}\right) = I\left(1 - GF^{-1}\left(U_{(a:m)}\right), j, n-j+1\right), \quad (3)$$

respectively, where $I(.,.,.)$ denotes the incomplete beta function and $\Psi(u) = GF^{-1}\left(U_{(e:l)}\right)$ is the conversion function for any two continuous distributions G and F where $U_{(e:l)}$ represents the e^{th} order statistic of a sample of size l from the Uniform (0,1) distribution.

Note that Equations (1) - (3) do not depend on the parent cdfs, when the process is IC or $F = G$.

It is important to know that the process is IC if $G = F$. In this case, $\Psi(u) = GF^{-1}(u) = u$ for any $u \epsilon (0,1)$. For more details on the precedence scheme, the reader is referred to Chakraborti, Van der Laan, and Van de Wiel (2004); Chakraborti, Eryilmaz, and Human (2009); Balakrishnan, Paroissin, and Turlot (2015) and Malela- Majika, Chakraborti, and Graham (2016).

2.2 The generalized 2-of-(h+1) DR and KL Shewhart-type precedence schemes:

2.2.1. Transition probability matrices (TPMs)

Before introducing the general results, we first discuss how to obtain the TPMs of the 2-*of*-(*h*+1) KL and DR schemes when *h* = 2. To construct the TPMs, we need to define the compound pattern denoted Λ that results in an OOC event – this procedure is also used in Shongwe and Graham (2016). Let us consider the compound pattern Λ ={11, 121, 33, 323}. For example, '323' indicates that in a sequence of three test samples, the first and third samples are lower non-conforming samples (i.e. plot in Zone 3 – see Figure 1), and the second is a conforming sample (i. e. plots in Zone 2). The elements, 11, 121, 33 and 323 in the compound pattern Λ show all possible ways of obtaining and OOC signal using the 2-*of*-(*h*+1) KL scheme. The Markov chain states of the 2-*of*-(*h*+1) KL scheme, based on the compound pattern Λ when *h* = 2, are obtained as follows (see Table 1):

Step 1: List all the elements in the compound pattern Λ. In our example Λ = {11, 121, 33, 323}.

Step 2: Create the dummy state denoted ϕ which is defined by the single IC state given by {2}. This IC state can also be denoted by $\eta_{h+1} = \phi$. Thus, when *h* = 2, $\eta_3 = \phi$= {2}.

Step 3: Decompose each element of the compound pattern given in Step 1 into its basic (i.e. transient sub-patterns) states by removing the last nonconforming element. These sub-patterns are non-absorbing states denoted by η_1 η_2 η_4 and η_5. For example, the element '323' is decomposed into a transient state '32'. Decomposing all elements in Λ give the complete set of the basic states denoted by η. Therefore, when *h* = 2, η = {12, 1, 3, 32} where the basic states are defined as η_1 = {12},

$\eta_2 = \{1\}$, $\eta_4 = \{3\}$ and $\eta_5 = \{32\}$. Note that the sub-pattern η_3 (i.e. η_{h+1}), which is also non-absorbing, is defined in Step 2.

Step 4: Denote the OOC states in Step 1 as "OOC". For example, for h = 2, OOC = {11, 121, 33, 323}.

Step 5: Combine the states in Steps 2 to 4 to get the state space denoted by $\mathbf{\Omega}$. Hence, when h = 2, the state space of the 2-*of*-(h+1) KL scheme is given by $\mathbf{\Omega} = \{\eta_1, \eta_2, \eta_3 = \phi, \eta_4, \eta_5;$ OOC}. The number of non-absorbing sub-patterns from the state space is denoted by τ. Therefore, the essential TPM of the proposed scheme is a $\tau \times \tau$ matrix {where τ = 2h + 1). When h = 2, τ = 5. For illustration purpose, in Table 1, the state space $\mathbf{\Omega}$ is constructed for h = 1, 2, 3 and 4 for the KL schemes.

Step 6: Construct the TPMs of the proposed KL schemes as shown in Table 2 when h = 1, 2 and 3.

Table 1. Decomposition of the TPM's state space of a two-sided 2-*of*-(h+1) DR and KL schemes when h = 1, 2, 3 & 4

h	Scheme	Λ	ϕ	η	Ω
1	*DR	Λ_1={00}	η_1={2}	η_2={0}	{ϕ;η_2;OOC}
	KL	Λ_1={11}, Λ_2={33}	η_2={2}	η_1={1}, η_3={3}	{η_1; ϕ;η_3;OOC}
2	*DR	Λ_1={00}, Λ_2={020}	η_1={2}	η_2={0}, η_3={02}	{ϕ;η_2,η_3;OOC}
	KL	Λ_1={11}, Λ_2={121}, Λ_3={33}, Λ_4={323}	η_3={2}	η_1={12},η_2={1}, η_4={3},η_5={32}	{η_1,η_2;ϕ;η_4,η_5;OOC}
3	*DR	Λ_1={00}, Λ_2={020}, Λ_3={0220}	η_1={2}	η_2={2}, η_3={02}, η_4={022}	{ϕ;η_2,η_3,η_4;OOC}
	KL	Λ_1={11}, Λ_2={121}, Λ_3={1221}, Λ_4={33}, Λ_5={323}, Λ_6={3223}	η_4={2}	η_1={122}, η_2={12}, η_3={1}, η_5={3}, η_6={32}, η_7={322}	{η_1,η_2,η_3;ϕ;η_5,η_6,η_7;OOC}
4	*DR	Λ_1={00}, Λ_2={020}, Λ_3={0220}, Λ_4={02220}	η_1={2}	η_2={0}, η_3={02} η_4={022}, η_5={0222}	{ϕ;η_2,η_3, η_4,η_5;OOC}
	KL	Λ_1={11}, Λ_2={121}, Λ_3={1221}, Λ_4={12221}, Λ_5={33}, Λ_6={323}, Λ_7={3223}, Λ_8={32223}	η_5={2}	η_1={1}, η_2={12}, η_3={122}, η_4={1222}, η_6={3}, η_7={32}, η_8={322}, η_9={3222}	{η_1,η_2,η_3,η_4;ϕ;η_6,η_7,η_8,η_9;OOC}

*Note: for the DR scheme, Zone 0 = Zone 1 ∪ Zone 3 = (-∞, LCL] ∪ [UCL, + ∞).

Let us now consider the Markov chain states of the 2-*of*-(h+1) DR scheme based on the compound pattern Λ when h = 2. In this case, the compound pattern is given by Λ = {11, 121, 33, 323, 123, 13, 31, 321}. Accordingly to the DR scheme properties, and in order to simplify the compound pattern, we denote Zone 0 = Zone 1 ∪ Zone 3 since the DR scheme is a non-side-sensitive scheme. Hence, we assume that state 1 and state 3 represent the non-conforming state denoted by state 0. Therefore, the compound pattern becomes Λ = {00, 020, 00, 020, 020, 00, 00, 020} which is simplified into Λ = {00, 020}. Thus, the Markov chain states, of the 2-*of*-(h+1) DR scheme for h = 2, based on the simplified compound pattern are obtained as follows (see Table 1):

Step 1: List all the elements in the compound pattern Λ. In our example $\Lambda = \{00, 020\}$.

Step 2: Create the dummy state denoted ϕ which is defined by the single IC state given by $\{2\}$. To simplify the notation, the dummy (i.e. single IC) state will be denoted as $\eta_1 = \phi = \{2\}$ in Step 5.

Step 3: Decompose each element of the compound pattern given in Step 1 into its basic (i.e. transient sub-patterns) states by removing the last nonconforming element. These sub-patterns are non-absorbing states denoted by η_2 and η_3. Note that the sub-pattern η_1 which is also non-absorbing, is defined in Step 2. In our example for $h = 2$, $\eta_2 = \{0\}$ and $\eta_3 = \{02\}$.

Step 4: Denote the OOC states in Step 1 as "OOC". For example, for $h = 2$, OOC = {00, 020}.

Step 5: Combine the states in Steps 2 to 4 to get the state space denoted by $\mathbf{\Omega}$. Hence, when $h = 2$, the state space of the 2-*of*-(h+1) DR scheme is given by $\mathbf{\Omega} = \{\eta_1 = \phi, \eta_2, \eta_3;$ OOC$\}$. Therefore, the essential TPM of the proposed DR scheme is a $\tau \times \tau$ matrix {where $\tau = h + 1$). When $h = 2$, $\tau = 3$. For illustration purpose, in Table 1, the state space $\mathbf{\Omega}$ is constructed for h = 1, 2, 3 and 4 for the DR schemes.

Step 6: Construct the TPMs of the proposed DR schemes as shown in Table 2.

For more details on how to construct the TPMs of the 2-*of*-(h+1) KL and DR schemes, readers are referred to Shongwe and Graham (2016, 2017).

Table 2 presents the TPMs of the 2-*of*-(h+1) KL and DR schemes when h = 1, 2 and 3 where p_1, p_2 and p_3 are computed using Equations (1)-(3), respectively, and $p_0 = p_1 + p_3$.

Table 2. TPMs of the two-sided 2-*of*-(*h*+1) DR and KL schemes when *h* = 1, 2 and 3

h = 1, DR scheme

	ϕ	η_2	OOC
ϕ	p_2	p_0	0
η_2	p_2	0	p_0
OOC	0	0	1

h = 1, KL scheme

	η_1	ϕ	η_3	OOC
η_1	0	p_2	p_3	p_1
ϕ	p_1	p_2	p_3	0
η_3	p_1	p_2	0	p_3
OOC	0	0	0	1

h = 2, DR scheme

	ϕ	η_2	η_3	OOC
ϕ	p_2	p_0	0	0
η_2	0	0	p_2	p_0
η_3	p_2	0	0	p_0
OC	0	0	0	1

h = 2, KL scheme

	η_1	η_2	ϕ	η_4	η_5	OOC
η_1	0	0	p_2	p_3	0	p_1
η_2	p_2	0	0	p_3	0	p_1
ϕ	0	p_1	p_2	p_3	0	0
η_4	0	p_1	0	0	p_2	p_3
η_5	0	p_1	p_2	0	0	p_3
OOC	0	0	0	0	0	1

h = 3, DR scheme

	ϕ	η_2	η_3	η_4	OOC
ϕ	p_2	p_0	0	0	0
η_2	0	0	p_2	0	p_0
η_3	0	0	0	p_2	p_0
η_4	p_2	0	0	0	p_0
OOC	0	0	0	0	1

h = 3, KL scheme

	η_1	η_2	η_3	ϕ	η_5	η_6	η_7	OOC
η_1	0	0	0	p_2	p_3	0	0	p_1
η_2	p_2	0	0	0	p_3	0	0	p_1
η_3	0	p_2	0	0	p_3	0	0	p_1
ϕ	0	0	p_1	p_2	p_3	0	0	0
η_5	0	0	p_1	0	0	p_2	0	p_3
η_6	0	0	p_1	0	0	0	p_2	p_3
η_7	0	0	p_1	p_2	0	0	0	p_3
OOC	0	0	0	0	0	0	0	1

Note: $p_0 = p_1 + p_3$ (since Zone 0 = Zone 1 ∪ Zone 3)

3. Run-length distribution of the 2-*of*-(*h*+1) schemes

The characteristics of the run-length distribution reveal important information about the performance of a control chart. In this section, we give the expressions of the run-length distribution of the proposed schemes.

The TPM of a two-sided 2-*of*-(*h*+1) DR scheme using Markov chain approach for any integer τ is given by

$$\boldsymbol{P}_{(\tau+1)\times(\tau+1)} = \begin{pmatrix} \boldsymbol{Q}_{\tau\times\tau} & | & \boldsymbol{r}_{\tau\times1} \\ - & - & - \\ \boldsymbol{0}'_{1\times\tau} & | & 1_{1\times1} \end{pmatrix} \tag{4}$$

where $\boldsymbol{Q} = \boldsymbol{Q}_{\tau\times\tau}$ is the essential TPM of the chart, $\boldsymbol{r} = \mathbf{1} - \boldsymbol{Q}\mathbf{1}$ with $\boldsymbol{r} = \boldsymbol{r}_{\tau\times1}$, $\mathbf{0}_{\tau\times1} = (0\ 0\ ...\ 0)'$ and $\mathbf{1} = \mathbf{1}_{\tau\times1} = (1\ 1\ ...\ 1)'$. Note that Equation (4) is very important in the derivation of the properties (or characteristics) of the run-length using the Markov chain technique (see Fu and Lou (2003)). Thus, the conditional run-length (CRL) distribution and *ARL* of the 2-*of*-(*h*+1) schemes are given by

$$\boldsymbol{P}(N = t) = \boldsymbol{\xi}\, \boldsymbol{Q}^{t-1}(\mathbf{I} - \boldsymbol{Q})\mathbf{1} \text{ for } t = 1, 2, 3, ... \text{ with } \boldsymbol{Q}^0 = \mathbf{I} \tag{5}$$

and

$$\boldsymbol{CARL} = \boldsymbol{\xi}\,\mathbf{R} \tag{6}$$

respectively, where $\mathbf{I} = \mathbf{I}_{\tau\times\tau}$ and $\boldsymbol{\xi} = \boldsymbol{\xi}_{1\times\tau}$ is the initial probability vector and $\mathbf{R} = (\mathbf{I} - \boldsymbol{Q})^{-1}\mathbf{1}$ is the $\tau \times 1$ *CARL* vector.

Therefore, the unconditional *ARL* (*UARL*) is then defined by

$$\boldsymbol{UARL} = \int_0^1 \int_0^t \boldsymbol{CARL}\, f_{ab}(s,t)dsdt \tag{7}$$

where $f_{ab}(s,t) = \frac{m!}{(a-1)!\,(b-a-1)!(m-b)!} t^{a-1}(t-s)^{b-a-1}(1-t)^{m-b}$ which is the joint pdf of the a^{th} and b^{th} order statistics in a random sample of size *m* from the Uniform (0,1) distribution, *s* and *t* are random variables from the Uniform (0,1) distribution.

Note that in order to compute Equations (5)-(7), the initial probability vector (i.e. $\boldsymbol{\xi}$) has to be defined. In the zero-state mode we have $\boldsymbol{\xi} = \boldsymbol{q} = (1\ 0\ 0\ \ldots 0)$ for the 2-*of*-(*h*+1) DR scheme. The zero-state initial probability vector of the 2-*of*-(*h*+1) KL scheme is given by $\boldsymbol{\xi} = \boldsymbol{q} = (0\ \ldots\ 0\ 1\ 0\ \ldots\ 0)$ where the unique "1" is located at the $\frac{\tau+1}{2}^{th}$ position. However, in the steady-state mode, $\boldsymbol{\xi} = \boldsymbol{s} = (s_1, s_2, s_3, \ldots, s_\tau)$ which is obtained by dividing each element of $\boldsymbol{Q}(\delta = 0)$ by its corresponding row sum, so that the new essential TPM $\boldsymbol{Q}$ called the conditional essential TPM, denoted by $\boldsymbol{Q_C}$ is ergodic (i.e. $\boldsymbol{s}^{\mathrm{T}}\boldsymbol{Q_C} = \boldsymbol{s}^{\mathrm{T}}$ subject to $\sum_{j=1}^{\tau} \boldsymbol{s}_j = 1$). Therefore, the zero-state initial probability vectors of the 2-*of*-(*h*+1) DR and KL schemes are given by

$$\boldsymbol{q}_{1\times\tau} = (1\ 0\ 0\ \ldots 0) \tag{8a}$$

and

$$\boldsymbol{q}_{1\times\tau} = \left(0\ 0\ 0 \ldots 1_{\frac{\tau+1}{2}}\ \ldots 0\ 0\right) \tag{8b}$$

respectively.

However, the steady-state initial probability vector of the 2-*of*-(*h*+1) DR and KL schemes are given by

$$\boldsymbol{s}_{1\times\tau} = \frac{1}{1+h\,p_0}\ (1\ p_0\ p_0\ \ldots\ p_0) \tag{9a}$$

and

$$\mathbf{s}_{(1\times\tau)} = \begin{pmatrix} s_1 \\ s_2 \\ s_3 \\ \vdots \\ s_{h-2} \\ s_{h-1} \\ s_h \\ s_{h+1} \\ s_{h+2} \\ s_{h+3} \\ s_{h+4} \\ \vdots \\ s_{2h-1} \\ s_{2h} \\ s_{2h+1} \end{pmatrix}' = \frac{1}{2\sum_{i=0}^{h-1}\theta^i + 2\theta^h(1-p_2)^{-1}} \begin{pmatrix} \theta^{h-1} \\ \theta^{h-2} \\ \theta^{h-3} \\ \vdots \\ \theta^2 \\ \theta \\ 1 \\ 2\theta^h(1-p_2)^{-1} \\ 1 \\ \theta \\ \theta^2 \\ \vdots \\ \theta^{h-3} \\ \theta^{h-2} \\ \theta^{h-1} \end{pmatrix}' \quad (9b)$$

respectively, with $p_0 = p_1 + p_3$, $\theta = \frac{2p_2}{1+p_2}$ and p_2 is defined in Equation (2).

3.1 Zero-state and steady-state run-length characteristics of the 2-of-(h+1) DR schemes

The zero-state and steady-state modes are mostly used to characterize the short-term and the long-term run-length properties of a scheme. The zero-state run-length is defined as the number of sampling points at which the chart first signals given that it begins in some specific initial state. However, the steady-state run-length is the number of sampling points at which the chart first signals given that the process begins and stays IC for a long time, then at some random time, an OOC is observed.

Equation (4) of the 2-*of*-(*h*+1) DR schemes for any value of *h* is given by

	ϕ	η_2	η_3	η_4	$\cdots$	η_{h+1}	OOC
ϕ	p_2	p_0	0	0	$\cdots$	0	0
η_2	0	0	p_2	0	$\cdots$	0	p_0
η_3	0	0	0	p_2	$\cdots$	0	p_0
$\vdots$	$\vdots$	$\vdots$	$\vdots$	$\vdots$	$\ddots$	$\vdots$	$\vdots$
η_h	0	0	0	0	$\cdots$	p_2	p_0
η_{h+1}	p_2	0	0	0	$\cdots$	0	p_0
OOC	0	0	0	0	$\cdots$	0	1

where $\tau = h + 1$ and $p_0 = p_1 + p_3$. For both zero- and steady-state modes, the *CARL* vector (i.e. $\mathbf{R}_{\tau\times 1}$) of the 2-*of*-(*h*+1) DR scheme for any value of *h* is given by

$$\mathbf{R}_{\tau\times 1}(\delta)=\begin{pmatrix}\zeta_1(\delta)\\ \zeta_2(\delta)\\ \zeta_3(\delta)\\ \zeta_4(\delta)\\ \vdots\\ \zeta_{h-2}(\delta)\\ \zeta_{h-1}(\delta)\\ \zeta_h(\delta)\\ \zeta_{h+1}(\delta)\end{pmatrix}=\frac{1}{1-p_2-p_2^h+p_2^{h+1}}\begin{pmatrix}2-p_2^h\\ 1\\ 1+p_2^{h-1}-p_2^h\\ 1+p_2^{h-2}-p_2^h\\ \vdots\\ 1+p_2^4-p_2^h\\ 1+p_2^3-p_2^h\\ 1+p_2^2-p_2^h\\ 1+p_2-p_2^h\end{pmatrix} \quad (10)$$

Substituting Equations (8a) and (10) into Equations (6) and (7), the conditional zero-state *ARL* (denoted as $CARL_{ZS}$) of the two-sided 2-*of*-(h+1) DR scheme for any value of h is given by

$$CARL_{ZS}(\delta)=\frac{2-p_2^h}{1-\ p_2-p_2^h-\ p_2^{h+1}}. \quad (11)$$

where p_2 is defined in Equation (2).

The unconditional zero-state *ARL* (denoted as $UARL_{ZS}$) is then defined by

$$UARL_{ZS}(\delta)=\int_0^1\int_0^t\left[\frac{2-p_2^h}{1-\ p_2-p_2^h-\ p_2^{h+1}}\right] f_{ab}\,(s,t)ds\,dt \quad (12)$$

where $f_{ab}(s,t)$ is defined in Equation (7).

However, substituting Equations (9a) and (10) into Equations (6) and (7), the conditional steady-state *ARL* (denoted as $CARL_{SS}$) of the two-sided 2-*of*-(h+1) DR scheme for any value of h is given by

$$CARL_{SS}(\delta)=\frac{1}{1+h\,p_0}\zeta_1(\delta)+\frac{p_0}{1+h\,p_0}\sum_{i=2}^{h+1}\zeta_i(\delta). \quad (13)$$

Therefore, the unconditional steady-state *ARL* ($UARL_{SS}$) is given by

$$UARL_{SS}(\delta)=\int_0^1\int_0^t\left[\frac{1}{1+h\,p_0}\zeta_1(\delta)+\frac{p_0}{1+h\,p_0}\sum_{i=2}^{h+1}\zeta_i(\delta)\right]f_{ab}(s,t)\,dsdt \quad (14)$$

where the components of the *CARL* vector (i.e. ζ_i) are defined in Equation (10).

3.2 *Zero-state and steady-state run-length characteristics of the 2-of-(h+1) KL schemes*

Following a similar procedure as done in Shongwe and Graham (2017), the TPM of the two-sided 2-*of*-(h+1) KL scheme in Equation (4) for any value of h is given by

	η_1	η_2	$\cdots$	η_{l-4}	η_{l-3}	η_{l-2}	η_{l-1}	ϕ	η_{l+1}	η_{l+2}	η_{l+3}	η_{l+4}	$\cdots$	$\eta_{\tau-2}$	$\eta_{\tau-1}$	η_τ	OOC
η_1								p_2	p_3								p_1
η_2	p_2								p_3								p_1
η_3		p_2							p_3								p_1
$\vdots$			$\ddots$						$\vdots$								$\vdots$
η_{l-3}				p_2					p_3								p_1
η_{l-2}					p_2				p_3								p_1
η_{l-1}						p_2			p_3								p_1
ϕ							p_1	p_2	p_3								
η_{l+1}							p_1			p_2							p_3
η_{l+2}							p_1				p_2						p_3
η_{l+3}							p_1					p_2					p_3
$\vdots$							$\vdots$						$\ddots$				$\vdots$
$\eta_{\tau-3}$							p_1							p_2			p_3
$\eta_{\tau-2}$							p_1								p_2		p_3
$\eta_{\tau-1}$							p_1									p_2	p_3
η_τ							p_1	p_2									p_3
OOC																	1

where $l = \frac{\tau+1}{2}$ and $\tau = 2h + 1$.

For both zero- and steady-state modes, the *CARL* vector of the 2-*of*-(h+1) KL scheme for any value of h is defined by

$$\mathbf{R}_{(\tau\times 1)}(\delta)=\begin{pmatrix}\zeta_1(\delta)\\ \zeta_2(\delta)\\ \vdots\\ \zeta_{h-3}(\delta)\\ \zeta_{h-2}(\delta)\\ \zeta_{h-1}(\delta)\\ \zeta_h(\delta)\\ \zeta_{h+1}(\delta)\\ \zeta_{h+2}(\delta)\\ \zeta_{h+3}(\delta)\\ \zeta_{h+4}(\delta)\\ \zeta_{h+5}(\delta)\\ \vdots\\ \zeta_{2h}(\delta)\\ \zeta_{2h+1}(\delta)\end{pmatrix}=\frac{1}{1-p_2-p_1p_2^h-p_3p_2^h-p_1p_3\sum_{i=0}^{2h-1}p_2^i}\begin{pmatrix}\left(1+p_1p_2\sum_{i=0}^{h-2}p_2^i\right)\left(1+p_3\sum_{i=0}^{h-1}p_2^i\right)\\ \left(1+p_1p_2^2\sum_{i=0}^{h-3}p_2^i\right)\left(1+p_3\sum_{i=0}^{h-1}p_2^i\right)\\ \vdots\\ \left(1+p_1p_2^{h-3}\sum_{i=0}^{2}p_2^i\right)\left(1+p_3\sum_{i=0}^{h-1}p_2^i\right)\\ \left(1+p_1p_2^{h-2}\sum_{i=0}^{1}p_2^i\right)\left(1+p_3\sum_{i=0}^{h-1}p_2^i\right)\\ (1+p_1p_2^{h-1})\left(1+p_3\sum_{i=0}^{h-1}p_2^i\right)\\ 1+p_3\sum_{i=0}^{h-1}p_2^i\\ \left(1+p_1\sum_{i=0}^{h-1}p_2^i\right)\left(1+p_3\sum_{i=0}^{h-1}p_2^i\right)\\ 1+p_1\sum_{i=0}^{h-1}p_2^i\\ (1+p_3p_2^{h-1})\left(1+p_1\sum_{i=0}^{h-1}p_2^i\right)\\ \left(1+p_3p_2^{h-2}\sum_{i=0}^{1}p_2^i\right)\left(1+p_1\sum_{i=0}^{h-1}p_2^i\right)\\ \left(1+p_3p_2^{h-3}\sum_{i=0}^{2}p_2^i\right)\left(1+p_1\sum_{i=0}^{h-1}p_2^i\right)\\ \vdots\\ \left(1+p_3p_2^2\sum_{i=0}^{h-3}p_2^i\right)\left(1+p_1\sum_{i=0}^{h-1}p_2^i\right)\\ \left(1+p_3p_2\sum_{i=0}^{h-2}p_2^i\right)\left(1+p_1\sum_{i=0}^{h-1}p_2^i\right)\end{pmatrix} \quad (15)$$

Substituting Equations (8b) and (15) into Equations (6) and (7), the $UARL_{ZS}$ of the two-sided 2-*of*-(h+1) KL scheme for any value of h is given by

$$UARL_{ZS}(\delta)=\int_0^1\int_0^t\left[\frac{\left(1+p_1\sum_{i=0}^{h-1}p_2^i\right)\left(1+p_3\sum_{i=0}^{h-1}p_2^i\right)}{1-p_2-p_1p_2^h-p_3p_2^h-p_1p_3\sum_{i=0}^{2h-1}p_2^i}\right]f_{ab}\,(s,t)ds\;dt \quad (16)$$

However, substituting Equations (9b) and (15) into Equations (6) and (7), the $UARL_{SS}$ of the two-sided 2-*of*-(h+1) KL scheme for any value of h is given by

$$UARL_{SS}(\delta) = \int_0^1 \int_0^t \left[s_{h+1}\zeta_{H+1}(\delta) + \sum_{i=1}^{h} s_i \times \left(\zeta_i(\delta) + \zeta_{(2h+2)-i}(\delta)\right)\right] f_{ab}\,(s,t)ds\,dt, \qquad (17)$$

where the components of the steady-state initial vector $\boldsymbol{s}$ are defined in Equation (9b) and ζ_i are the components of the *CARL* vector defined in Equation (15).

3.3 Overall performance measure

Many studies in SPCM use the ARL values to assess the performance of schemes (Li et al., 2014). This measure evaluates the performance of a control chart for a specific shift. Therefore, schemes which are designed on the basis of a specified optimal shift (say, δ_{opt}) will perform poorly if the shift is actually different from δ_{opt}. When researchers are interested in measuring the chart's performance for a range of shifts, $\delta_{min} \leq \delta \leq \delta_{max}$, it is recommended to use measures of the overall performance (Machado and Costa, 2014). In this paper, we make use of one of the characteristics of the quality loss function (*QLF*), the average extra quadratic loss (*AEQL*) value, in order to investigate the overall performance of the proposed schemes. A *QLF* describes the relationship between the size of the shift and the quality impact. For more details on the overall measures of performance, readers are referred to Wu et al. (2008) and Reynolds and Lou (2010).

Writing $f(\delta)$ as the pdf of a uniform distribution with parameters 0 and 1, the *AEQL* may be given by:

$$AEQL = \frac{1}{\delta_{max} - \delta_{min}} \int_{\delta_{min}}^{\delta_{max}} \left(\delta^2 \times ARL(\delta)\right) \times f(\delta)d\delta. \qquad (18)$$

When comparing several schemes, the scheme with the minimum *AEQL* value is considered to be the winner.

4. Zero-state and steady-state performance studies of the 2-*of*-(*h*+1) precedence schemes

4.1 Design of the proposed control charts

One of the most important steps in the design and implementation of a scheme is the computation (or search) of the control limits. The control limits of the 2-*of*-(*h*+1) precedence schemes are determined once the plotting constants a and b (with $b = m - a + 1$) are found.

The plotting constants denote the position of the order statistics in the Phase I sample. For instance, the zero-state plotting constants of the 2-*of*-(h+1) DR and KL precedence schemes are determined using Equations (12) and (16), respectively, whereas the steady-state plotting constants are found using Equations (14) and (17), respectively, so that the IC $UARL_{ZS}$ ($UARL_{0ZS}$) and $UARL_{SS}$ ($UARL_{0SS}$) are equal (or close) to some high desired values such as 370 or 500. For example, for m = 200 and n = 5 so that j = 3 and for a nominal IC ARL (ARL_0) of 370, it is found that the couple (a, b) = (31, 170) yields an attained $UARL_{0ZS}$ of 368.78, so that ($\widehat{LCL}$, $\widehat{UCL}$) of the zero-state 2-*of*-2 DR precedence scheme is given by $(X_{(31:200)}, X_{(170:200)})$ when h = 1. On the other hand, with the same settings, it is found that for the zero-state KL case, when h = 1, the couple (a, b) = (34, 167) so that ($\widehat{LCL}$, $\widehat{UCL}$) = $(X_{(34:200)}, X_{(167:200)})$ which yields an attained $UARL_{0\ ZS}$ of 399.6 (see Table 3). Table 3 gives the 2-*of*-(h+1) DR and KL plotting constants (a, b) as well as the attained $UARL_{0ZS}$ and $UARL_{0SS}$ values for h = 1, 2, 5 and 10 when m = 100, 200 and 500 with n = 5 and 7. The first row of each cell in Table 3 is related to a nominal $UARL_{0ZS}$ and $UARL_{0SS}$ value of 370, whereas the second row is related to a nominal $UARL_{0ZS}$ and $UARL_{0SS}$ value of 500.

Table 3. Zero-state and steady-state plotting constants (a, b) and the attained $UARL_{0ZS}$ and $UARL_{0SS}$ values of the 2-*of*-(h+1) DR and KL precedence schemes under the N(0,1), t(5) and GAM(1,1) distributions when h = 1, 2, 5 and 10 for a nominal ARL_0 of 370 & 500.

h	**m**	**DR**								**KL**							
		n = 5, j = 3				**n = 7, j = 4**				**n = 5, j = 3**				**n = 7, j = 4**			
		a	**b**	**$UARL_{0ZS}$**	**$UARL_{0SS}$**	**a**	**b**	**$UARL_{0ZS}$**	**$UARL_{0SS}$**	**a**	**b**	**$UARL_{0ZS}$**	**$UARL_{0SS}$**	**a**	**b**	**$UARL_{0ZS}$**	**$UARL_{0SS}$**
1	100	16	85	373.31	372.38	20	81	345.93	345.00	18	83	328.69	327.84	21	80	414.67	413.84
		15	86	548.99	548.04	19	82	509.54	508.60	17	84	456.52	455.67	20	81	594.56	593.73
	200	31	170	368.78	367.84	39	162	336.98	336.04	34	167	399.6	398.71	42	159	358.81	357.93
		29	172	537.62	536.67	37	164	490.44	489.49	33	168	471.18	470.29	40	161	504.01	503.13
	500	76	425	369.50	368.55	94	407	388.83	387.88	85	416	377.91	376.98	104	397	362.28	361.36
		72	429	496.89	495.94	90	411	526.08	525.12	81	420	490.21	489.28	99	402	506.61	505.69
2	100	14	87	437.09	435.71	18	83	404.63	403.26	16	85	342.26	341.02	20	81	313.2	311.99
		13	88	686.85	685.45	17	84	628.91	627.51	15	86	498.01	496.77	19	82	456.58	455.37
	200	28	173	346.51	345.13	35	166	385.72	384.34	31	170	351.66	350.35	38	163	380.70	379.42
		26	175	526.40	525.00	34	167	474.78	473.39	29	172	507.88	506.57	37	164	458.64	457.35
	500	68	433	359.81	358.41	86	415	381.59	380.19	76	425	365.41	364.04	94	407	381.07	379.71
		64	437	500.71	499.30	83	418	488.05	486.64	72	429	488.49	487.11	90	411	512.46	511.10
5	100	13	88	303.31	300.58	17	84	278.44	275.74	14	87	330.1	327.76	18	83	302.52	300.23
		12	89	489.80	486.99	16	85	440.34	437.57	13	88	508.34	505.98	17	84	461.12	458.82
	200	24	177	367.45	364.63	31	170	408.67	405.84	27	174	335.06	332.56	34	167	368.11	365.65
		23	178	466.02	463.16	30	171	518.78	513.91	25	176	509.83	507.31	33	168	452.82	450.35
	500	58	443	381.30	378.43	77	424	366.04	363.18	65	436	375.96	373.32	84	417	364.57	361.96
		55	446	507.27	504.37	74	427	480.3	477.40	62	439	482.68	480.03	80	421	506.27	503.64
10	100	12	89	275.36	270.97	15	86	401.38	396.88	13	88	285.44	281.39	16	85	402.53	398.53
		11	90	460.28	455.70	14	87	687.1	682.44	12	89	451.04	446.93	15	86	655.21	651.15
	200	22	179	336.12	331.51	29	172	368.35	363.73	24	177	357.24	352.86	31	170	391.36	387.04
		21	180	433.28	428.58	28	173	471.06	466.36	23	178	448.61	444.20	30	171	490.33	485.98
	500	52	449	385.30	380.56	71	430	359.3	354.60	58	443	385.42	380.76	77	424	367.88	363.28
		49	452	526.95	522.12	68	433	479.74	474.94	55	446	507.64	502.93	74	427	478.05	473.40

4.2 Robustness of the proposed control charts

The ARL_0 of the nonparametric scheme does not depend on the underlying process distribution. To check the robustness property of the proposed schemes, we consider various distributions. The standard normal distribution, $N(0,1)$, is used to investigate the effect of symmetric distributions, the Student's t-distribution, with degree of freedom 5, $t(5)$, to study the effect of heavy tails and the gamma distribution, $GAM(1,1)$, to investigate the effect of skewness. From Tables 3 and 4, it can be seen that, as expected, for every continuous distribution under consideration, the proposed schemes yield the same IC characteristics (i.e., $UARL_{0ZS}$ or $UARL_{0SS}$). For instance, we computed the control limits and the attained $UARL_{0SS}$ values for the 2-*of*-4 KL precedence scheme (i.e., when $h = 3$) under the $N(0,1)$, $t(5)$ and $GAM(1,1)$ distributions for $m = 500$, $n = 5$ and a nominal $UARL_{0SS}$ value of 500. We find that $(\widehat{LCL}, \widehat{UCL}) = (X_{(67:500)}, X_{(434:500)})$ yields a $UARL_{0SS}$ value of 497.48 under these three distributions (see Table 4). This shows that the proposed schemes are IC robust.

Table 4. Zero-state and steady-state *AEQL*, plotting constants (*a*, *b*) and the attained $UARL_{0ZS}$ ($UARL_{0SS}$) values of the Shewhart 2-*of*-(*h*+1) DR and KL precedence schemes for different values of *h* under the *N*(0,1), *t*(5) and *GAM*(1,1) distributions when *m* = 500 and *n* = 5.

	DR scheme								KL scheme							
h	**(a, b)**	$UARL_{0ZS}$ ($UARL_{0SS}$)	**Zero-state**			**Steady-state**			**(a, b)**	$UARL_{0ZS}$ ($UARL_{0SS}$)	**Zero-state**			**Steady-state**		
			N(0,1)	**t(5)**	**GAM(1,1)**	**N(0,1)**	**t(5)**	**GAM(1,1)**			**N(0,1)**	**t(5)**	**GAM(1,1)**	**N(0,1)**	**t(5)**	**GAM(1,1)**
1	(72, 429)	496.89 (495.94)	104.72	85.69	193.92	102.99	84.09	191.22	(81, 420)	490.21 (489.28)	92.88	78.64	169.49	91.7	77.55	167.7
2	(64, 437)	500.71 (499.30)	100.79	84.74	170.65	98.38	82.54	167.17	(72, 429)	488.49 (487.11)	90.12	77.97	151	88.48	76.42	148.69
3	(60, 441)	494.75 (492.89)	99.53	84.72	163.78	96.53	81.92	159.47	(67, 434)	499.00 (497.48)	90.08	78.42	147.33	88.08	76.54	144.5
4	(57, 444)	507.41 (505.11)	99.94	85.49	162.81	96.46	82.27	157.72	(64, 437)	494.79 (492.55)	90.03	78.67	146.15	87.68	76.48	142.78
5	(55, 446)	507.27 (504.37)	100.04	85.9	162.54	96.07	82.25	156.58	(62, 439)	482.68 (480.03)	89.9	78.78	145.78	87.23	76.28	141.85
6	(54, 447)	479.20 (476.05)	98.99	85.37	161.06	94.53	81.25	154.29	(60, 441)	491.41 (488.33)	90.54	79.37	147.15	87.61	76.64	142.75
7	(52, 449)	515.34 (511.76)	100.94	87.04	164.36	96.2	82.69	157.04	(58, 443)	516.06 (512.57)	91.74	80.34	149.59	88.61	77.44	144.81
8	(51, 450)	511.48 (507.48)	101.1	87.32	165.07	95.97	82.63	157.03	(57, 444)	505.78 (501.88)	91.78	80.46	150.13	88.38	77.32	144.86
9	(50, 451)	515.81 (511.39)	101.64	87.88	166.39	96.17	82.89	157.7	(56, 445)	503.53 (499.23)	92.09	80.75	151.12	88.45	77.41	145.42
10	(49, 452)	526.95 (522.12)	102.5	88.67	168.16	96.73	83.43	158.9	(55, 446)	507.64 (502.93)	92.6	81.19	152.46	88.76	77.67	146.36

4.3 OOC Performance

Since the proposed schemes are IC robust, it is of interest to compare their performance when the process is OOC. For a specific shift, $\delta \neq 0$, the scheme with a small OOC $UARL_{ZS}$ ($UARL_{\delta\ ZS}$) or small OOC $UARL_{SS}$ ($UARL_{\delta\ SS}$) value is considered to be more sensitive. When comparing the overall performance, the scheme with a small $AEQL$ is preferred. Note that, when δ_{max} = 0.7, the *AEQL* value gives the measure of the overall performance for small shifts only. When δ_{max} = 1.5, the *AEQL* value measures the overall performance for small and moderate shifts considered together. For δ_{max} = 3, the *AEQL* value measures the overall performance of small, moderate and large shifts considered together. In terms of the *UARL* value, under both zero-state and steady-state modes, Tables 5 and 6 showed that, for small shifts, the enhanced precedence DR schemes perform better under skewed distributions when h = 1. However, when h > 1, the 2-*of*-(h+1) DR scheme performs best under heavy tailed distributions followed by symmetric distributions. For moderate and large shifts, the proposed 2-*of*-(h+1) DR scheme performs best under heavy tailed distributions followed by symmetric distributions regardless of the value of h. Under heavy tailed distributions, for both zero-state and steady-state modes, the 2-*of*-(h+1) DR scheme performs better when h = 2 regardless of the size of the shift. However, under the symmetric distributions, the 2-*of*-(h+1) DR scheme performs better when h = 5. Under skewed distributions, for small and moderate shifts in the process mean, the proposed 2-*of*-(h+1) DR scheme performs better for large values of h. However, for large shifts, the 2-*of*-(h+1) DR scheme performs better when h = 5.

Tables 7 and 8 show that, for both zero-state and steady-state modes, the 2-*of*-(h+1) KL scheme performs better under heavy tailed distributions regardless of the size of the shift in the process mean. Moreover, for both zero-state and steady-state modes, for small shifts, the proposed 2-*of*-(h+1) KL scheme performs better under skewed distributions compared to symmetric distributions; whereas, for moderate and large shifts, the 2-*of*-(h+1) KL scheme performs better under symmetric distributions compared to skewed distributions. Under heavy tailed distributions, for both zero-state and steady-state modes, for very small shifts in the process mean, the proposed 2-*of*-(h+1) KL scheme performs better when $h = 5$ and for moderate to large shifts, the 2-*of*-(h+1) KL scheme performs better when $h = 2$. Under symmetric distributions, for small and moderate shifts, the 2-*of*-(h+1) KL scheme performs better when $h = 5$. For large shifts, the sensitivity of the 2-*of*-(h+1) KL scheme remains the same regardless of the value of h. Under skewed distributions, for small shifts, the 2-*of*-(h+1) KL scheme performs better for large values of h and for moderate and large shifts, the 2-*of*-(h+1) KL scheme performs better when $h=5$.

In terms of the *AEQL* values (i.e., overall performance), for δ_{max} = 0.7, the 2-*of*-(h+1) DR and KL precedence schemes are more sensitive under skewed distributions (see Figure 2a). For δ_{max} = 1.5 and δ_{max} = 3, the proposed schemes are more sensitive under heavy tailed distributions and insensitive under skewed distributions (see Figure 2b–2c).

When comparing the enhanced precedence schemes to the basic precedence scheme, we observe that, for δ_{max} = 0.7 and 1.5, the enhanced DR and KL precedence schemes outperform the basic precedence scheme (Figure 2a–2b). For δ_{max} = 3, under both zero-state and steady-state modes, the basic precedence scheme outperforms the 2-*of*-(h+1) DR precedence scheme regardless of the value of h under the symmetric and skewed distributions, whereas the enhanced DR precedence schemes outperform the basic precedence scheme under heavy tailed distributions. However, under the zero-state mode, the enhanced KL precedence schemes outperform the basic precedence scheme under symmetric and skewed distributions when h < 13 and, under heavy tailed distributions, the enhanced KL precedence schemes outperform the basic precedence scheme regardless of the value of h (Figure 2c). For δ_{max} = 3, under the steady-state mode, the enhanced KL precedence schemes outperforms the basic precedence scheme regardless of the value of h and the nature of underlying process distribution. Thus, the above dis- cussion indicates that adding runs-rules to the basic precedence scheme would not necessarily improve the efficiency of the scheme in some of the situations. The opera- tors would be advised to use these types of runs-rules only when small and moderate shifts are of interest. When large shifts are of interest, the operator would be advised to add runs-rules only for specific cases as above-mentioned.

The proposed 2-*of*-(h+1) KL precedence schemes perform better than the 2-*of*-(h+1) DR precedence schemes. This was expected according to the SPCM literature (Klein 2000). When comparing the zero-state and steady-state scheme performances, we observe that, for both DR and KL schemes, the steady-state performance of the proposed schemes is slightly better than the zero-state performance.

Table 5. Zero-state performance of the 2-of-(h+1) DR precedence scheme for h = 1, 2, 5, 10 and 15 when m = 500 and n = 5 for a nominal ARL_0 of 500

Shift(δ)	***N*(0,1)**					***t*(5)**					***GAM*(1,1)**				
0.1	433.20	431.78	432.41	446.23	449.79	413.73	415.12	420.24	437.80	443.71	348.78	339.39	330.29	334.35	334.23
0.2	298.80	289.79	282.22	286.91	287.97	254.18	252.03	254.46	266.98	272.90	224.71	210.14	195.89	193.38	191.70
0.3	178.79	167.94	158.77	159.31	159.70	132.11	128.95	129.80	137.53	142.28	142.76	128.78	115.89	112.47	111.16
0.4	101.61	92.89	86.10	86.08	86.72	65.79	63.29	63.76	68.46	71.86	92.96	81.51	71.65	69.04	68.41
0.5	58.22	52.26	48.14	48.46	49.34	33.86	32.25	32.72	35.73	38.12	63.03	54.16	47.03	45.36	45.22
0.6	34.67	30.84	28.57	29.17	30.11	18.67	17.71	18.21	20.25	21.93	44.66	37.87	32.77	31.80	31.96
0.7	21.73	19.29	18.12	18.84	19.71	11.20	10.63	11.10	12.55	13.74	33.00	27.76	24.09	23.59	23.90
0.8	14.37	12.82	12.27	12.99	13.75	7.32	6.98	7.40	8.45	9.30	25.31	21.22	18.53	18.34	18.73
0.9	10.03	9.02	8.81	9.48	10.12	5.20	4.99	5.35	6.12	6.71	20.06	16.81	14.81	14.81	15.23
1.0	7.36	6.69	6.67	7.27	7.78	3.97	3.84	4.14	4.70	5.11	16.36	13.72	12.21	12.33	12.76
1.5	2.88	2.78	2.91	3.12	3.25	2.19	2.18	2.25	2.34	2.40	7.98	6.84	6.40	6.69	7.01
2.0	2.13	2.12	2.17	2.22	2.25	2.02	2.01	2.02	2.03	2.04	5.26	4.63	4.50	4.75	4.95
3.0	2.00	2.00	2.00	2.00	2.00	2.00	2.00	2.00	2.00	2.00	3.42	3.13	3.15	3.30	3.39
AEQL	104.72	100.79	100.04	102.50	104.47	85.69	84.79	85.90	88.67	90.65	193.92	170.65	162.54	168.16	173.51
h	1	2	5	10	15	1	2	5	10	15	1	2	5	10	15

Table 6. Steady-state performance of the 2-of-(h+1) DR precedence scheme for h = 1, 2, 5, 10 and 15 when m = 500 and n = 5 for a nominal ARL_0 of 500

Shift(δ)	***N*(0,1)**					***t*(5)**					***GAM*(1,1)**				
0.1	432.31	430.47	429.74	441.82	443.57	412.87	413.84	417.62	433.44	437.55	347.98	338.23	327.97	330.55	328.90
0.2	298.07	288.73	280.10	283.44	283.10	253.51	251.05	252.47	263.67	268.22	224.08	209.23	194.13	190.55	187.78
0.3	178.23	167.14	157.22	156.80	156.21	131.63	128.26	128.43	135.24	139.05	142.25	128.07	114.56	110.38	108.28
0.4	101.19	92.31	84.99	84.30	84.26	65.45	62.82	62.83	66.92	69.69	92.55	80.96	70.64	67.46	66.24
0.5	57.90	51.83	47.34	47.19	47.58	33.62	31.92	32.09	34.69	36.64	62.70	53.71	46.23	44.12	43.52
0.6	34.43	30.51	27.97	28.23	28.80	18.50	17.48	17.76	19.51	20.88	44.39	37.50	32.12	30.80	30.59
0.7	21.54	19.04	17.67	18.12	18.71	11.07	10.45	10.77	12.00	12.96	32.76	27.45	23.55	22.75	22.76
0.8	14.23	12.62	11.92	12.42	12.96	7.22	6.84	7.15	8.02	8.70	25.11	20.95	18.07	17.62	17.75
0.9	9.91	8.86	8.53	9.02	9.48	5.11	4.87	5.14	5.77	6.24	19.88	16.57	14.41	14.18	14.37
1.0	7.26	6.56	6.43	6.88	7.24	3.90	3.74	3.97	4.41	4.72	16.20	13.52	11.86	11.78	12.00
1.5	2.83	2.70	2.78	2.91	2.98	2.14	2.11	2.14	2.18	2.19	7.87	6.70	6.17	6.32	6.51
2.0	2.09	2.05	2.06	2.06	2.05	1.97	1.95	1.92	1.89	1.86	5.18	4.52	4.32	4.46	4.57
3.0	1.95	1.94	1.90	1.86	1.83	1.95	1.93	1.90	1.86	1.83	3.35	3.05	3.01	3.08	3.11
AEQL	102.99	98.38	96.07	96.73	97.21	84.09	82.54	82.25	83.43	84.12	191.22	167.17	156.58	158.90	161.37
h	1	2	5	10	15	1	2	5	10	15	1	2	5	10	15

Table 7. Zero-state performance of the 2-*of*-(*h*+1) KL precedence scheme for *h* = 1, 2, 5, 10 and 15 when *m* = 500 and *n* = 5 for a nominal ARL_0 of 500

Shift(δ)	*N*(0,1)					*t*(5)					*GAM*(1,1)				
0.1	393.84	387.10	377.86	394.93	382.93	365.84	363.24	360.31	382.05	373.11	334.76	321.44	305.04	312.16	300.65
0.2	231.93	221.26	210.53	217.30	211.41	185.66	182.16	181.25	194.75	193.41	198.08	182.33	166.02	165.77	159.57
0.3	124.28	115.34	107.60	110.30	108.22	86.59	83.73	83.46	90.75	91.83	117.08	104.15	92.17	90.82	87.93
0.4	68.07	61.99	57.43	59.05	58.74	42.36	40.52	40.68	44.87	46.34	73.18	63.58	55.48	54.54	53.33
0.5	39.37	35.47	33.01	34.31	34.69	22.49	21.39	21.76	24.40	25.72	48.82	41.80	36.35	35.90	35.51
0.6	24.18	21.71	20.45	21.57	22.18	13.06	12.42	12.85	14.62	15.67	34.55	29.35	25.61	25.50	25.51
0.7	15.75	14.17	13.59	14.56	15.19	8.30	7.92	8.33	9.58	10.38	25.71	21.76	19.13	19.23	19.44
0.8	10.85	9.82	9.60	10.44	11.02	5.74	5.51	5.87	6.78	7.36	19.95	16.87	14.98	15.21	15.51
0.9	7.87	7.19	7.17	7.88	8.37	4.29	4.14	4.46	5.11	5.52	16.02	13.57	12.18	12.48	12.82
1.0	5.99	5.53	5.61	6.21	6.60	3.43	3.33	3.60	4.06	4.34	13.24	11.25	10.21	10.55	10.90
1.5	2.67	2.60	2.73	2.91	3.01	2.14	2.13	2.19	2.25	2.29	6.85	5.96	5.69	6.02	6.28
2.0	2.10	2.09	2.13	2.17	2.19	2.01	2.01	2.02	2.02	2.03	4.71	4.20	4.14	4.40	4.56
3.0	2.00	2.00	2.00	2.00	2.00	2.00	2.00	2.00	2.00	2.00	3.20	2.97	3.00	3.15	3.22
AEQL	92.88	90.12	89.90	92.60	93.79	78.64	77.97	78.78	81.19	82.27	169.49	151.00	145.78	152.46	156.55
h	1	2	5	10	15	1	2	5	10	15	1	2	5	10	15

Table 8. Steady-state performance of the 2-*of*-(*h*+1) KL precedence scheme for *h* = 1, 2, 5, 10 and 15 when *m* = 500 and *n* = 5 for a nominal ARL_0 of 500

Shift	*N*(0,1)					*t*(5)					*GAM*(1,1)				
0.1	393.05	385.95	375.66	391.06	377.46	365.09	362.14	358.19	378.28	367.76	334.02	320.37	303.03	308.66	295.75
0.2	231.38	220.49	209.09	214.81	207.91	185.19	181.48	179.95	192.45	190.13	197.55	181.59	164.68	163.48	156.39
0.3	123.92	114.83	106.68	108.73	106.03	86.30	83.31	82.67	89.37	89.87	116.70	103.63	91.26	89.29	85.82
0.4	67.81	61.64	56.81	58.00	57.28	42.17	40.25	40.18	43.99	45.09	72.89	63.20	54.82	53.45	51.84
0.5	39.18	35.22	32.57	33.56	33.66	22.36	21.21	21.42	23.81	24.87	48.60	41.51	35.85	35.08	34.38
0.6	24.04	21.52	20.12	21.02	21.41	12.96	12.28	12.60	14.20	15.06	34.37	29.11	25.21	24.85	24.61
0.7	15.64	14.02	13.33	14.13	14.59	8.22	7.81	8.14	9.26	9.92	25.56	21.56	18.80	18.70	18.70
0.8	10.76	9.70	9.40	10.09	10.53	5.68	5.42	5.72	6.52	7.00	19.82	16.70	14.70	14.75	14.88
0.9	7.80	7.09	7.00	7.60	7.97	4.24	4.07	4.33	4.90	5.23	15.91	13.43	11.93	12.08	12.27
1.0	5.93	5.45	5.47	5.97	6.27	3.38	3.27	3.49	3.88	4.10	13.14	11.12	9.99	10.20	10.41
1.5	2.63	2.55	2.64	2.77	2.83	2.10	2.08	2.11	2.14	2.16	6.78	5.88	5.54	5.78	5.96
2.0	2.06	2.04	2.05	2.06	2.06	1.98	1.96	1.94	1.92	1.90	4.65	4.13	4.02	4.21	4.31
3.0	1.97	1.95	1.93	1.90	1.88	1.97	1.95	1.93	1.90	1.88	3.15	2.91	2.91	3.00	3.03
AEQL	91.70	88.48	87.23	88.76	88.91	77.55	76.42	76.28	77.67	77.94	167.70	148.69	141.85	146.36	148.50
h	1	2	5	10	15	1	2	5	10	15	1	2	5	10	15

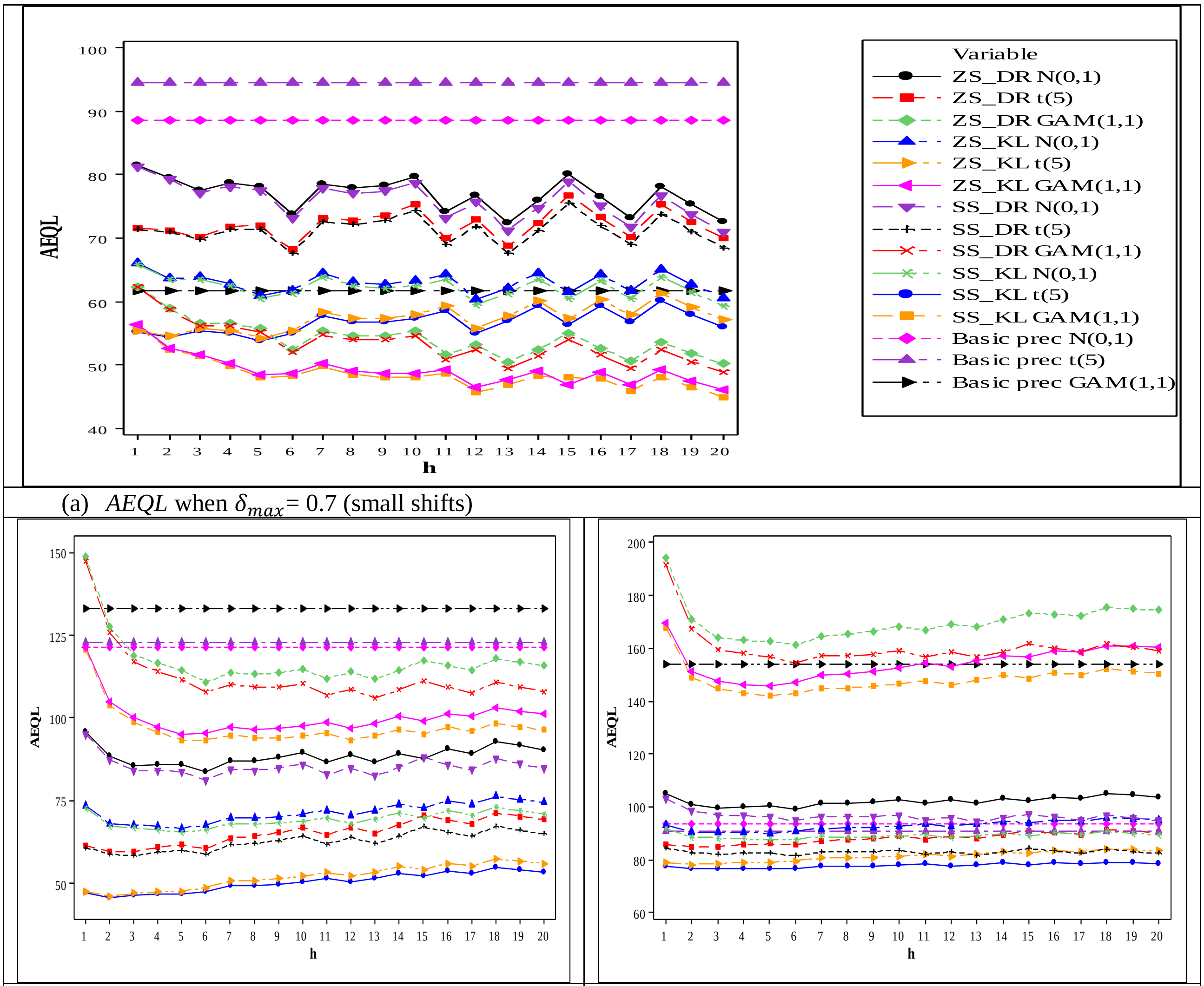

(a) *AEQL* when δ_{max}= 0.7 (small shifts)

(b) *AEQL* when δ_{max}= 1.5 (small & moderate shifts)

(c) *AEQL* when δ_{max}= 3 (small, moderate & large shifts)

Figure 2. Zero-state and steady-state overall performances of the 2-of-(h+1) DR/KL precedence and the basic precedence schemes when m = 500 and n = 5

5. Simulation studies

In this section, we use Monte Carlo simulations with 100000 replications to check the accuracy of the results obtained through the Markov chain approach. The Phase I sample size effect on the Phase II performance of the proposed schemes is also investigated through extensive simulations with 10000 replications.

5.1 Monte Carlo simulation

The plotting statistics and characteristics of the run-length distribution can also be obtained using the following steps:

Step 1: Specify the Phase I reference sample size (m), the Phase II test sample size (n), the number of simulations (r), the value of h and the parameter(s) of the distribution. For the IC case, the Phase I and Phase II distributions are identical. For instance, both distributions can be drawn from a $N(0,1)$ distribution (i.e., $\delta = 0$). For the OOC case, the Phase II distribution is taken to be the same form as that for the Phase I sample, but with a difference in the location parameter. In this case, if the Phase I is a $N(0,1)$ distribution, the Phase II will be a $N(\delta,1)$ distribution with δ from zero ($\delta \neq 0$).

Step 2: Set the plotting constant, a, to some integer value such that $1 \leq a < \frac{m}{2}$ and compute the corresponding value of b ($b = m - a + 1$). For example, when m = 100 and h = 2, we found $a = 64$ and $b = 437$ so that the attained ARL_0 is close or equal to 500.

Step 3: Generate a Phase I sample, X, from a distribution such as $N(0,1)$ distribution. The control limits are given by $LCL = X_{(a:m)}$ and $UCL = X_{(b:m)}$. In our example, $LCL = X_{(64:500)}$ and $UCL = X_{(437:500)}$.

Step 4: Randomly generate a Phase II test sample from the same distribution. In our example, the Phase II is generated from $N(\delta,1)$ distribution. Compute the plotting statistic $Y_{(j:n)}$ where $j = r + 1$ if $n = 2r + 1$ when n is odd. Compare the plotting statistic to the control limits obtained in Step 3. If this first point plots between the control limits (the process is IC) we have to generate the next test sample, compute the next plotting statistic and compare it to the control limits obtained in Step 3. Continue this process until two points out of $h + 1$ consecutive points plot beyond the control limits.

Step 5: The chart signals if: (i) the two points plot on or outside the control limits, no matter whether one (or both) plot(s) above the UCL and the other (or both) plot(s) below the LCL (DR scheme), and (ii) both points plot on or above (below) the UCL (LCL) (KL scheme). If (i) or (ii) does not happen according to the type of scheme (i.e., DR or KL scheme), then repeat Steps 4 and 5 until the chart signals for the first time and records the number of subgroups needed to get to that stage. This number represents one value of the run-length distribution.

Step 6: Repeat Steps 4 and 5 a total of r times.

Step 7: Once the unconditional run-length (URL) values are obtained, calculate: $UARL = \frac{1}{r}\sum_{i=1}^{r} URL_i$.

Step 8: For δ = 0, that is the IC case, if the ARL_0 value is much closer to the nominal value of 500, record the control limits (UCL and LCL). Otherwise, repeat Steps 2 to 7.

Step 9: Repeat Step 3 to 7 using the control limits found in Step 8 by varying the shift (δ = 0 (0.1) 3, where δ = 0 provides the IC values and $\delta \neq 0$ provides the OOC values). Record the IC and OOC *ARL* values.

A thorough examination of the results showed that the plotting constants and characteristics of the run-length distribution found using simulations are similar those found using Markov chain approach.

Let $UARL_{MC}$ denote the *UARL* values computed using the Markov chain approach and $UARL_{SIM}$ denote the *UARL* values computed using simulations. Table 9 displays the absolute percentage difference between the $UARL_{MC}$ and $UARL_{SIM}$ values. The absolute percentage difference is calculated as follows

$$\left|\frac{UARL_{MC} - UARL_{SIM}}{UARL_{MC}}\right| \tag{19}$$

For instance, in zero-state mode, when (m, n) = (500, 5), δ = 0 and h = 1, there is a 0.62% difference between the $UARL_{MC}$ and $UARL_{SIM}$ values of the DR scheme under the N(0,1) distribution. From Table 9 it can be observed that in the zero-state mode, under symmetric distributions, when h = 1, 2 and 5, there is a 0.63%, 1.18% and 1.43% (see boldfaced values in Table 9 - columns 2 to 4) difference between the $UARL_{MC}$ and $UARLS_{IM}$ values of the 2-*of*-(h+1) DR scheme, respectively. However, when h = 1, 2 and 5, there is a 0.67%, 1.21% and 1.44% difference between the $UARL_{MC}$ and $UARL_{SIM}$ values of the 2-*of*-(h+1) KL scheme, respectively. Under the heavy tailed distributions, when h = 1, 2 and 5, there is a 1.6%, 1.71% and 2.65% difference between the $UARL_{MC}$ and $UARL_{SIM}$ values of the 2-*of*-(h+1) DR scheme, respectively; whereas, there is a 1.89%, 1.94% and 2.81% difference between the $UARL_{MC}$ and $UARL_{SIM}$ values of the 2-*of*-(h+1) KL scheme. Under the skewed distributions, when h = 1, 2 and 5, there is a 2.36%, 3.04% and 3.12% difference between the $UARL_{MC}$ and $UARL_{SIM}$ values of the 2-*of*-(h+1) DR scheme, respectively, whereas there is a 2.76%, 2.98% and 3.01% difference between the $UARL_{MC}$ and $UARL_{SIM}$ values of the 2-*of*-(h+1) KL scheme. For both DR and KL schemes, the percentage difference between the $UARL_{MC}$ and $UARL_{SIM}$ values increases as (i) h

increases, and (ii) the distribution departs from normality. As we can see, there is not that much of a difference between $UARL_{MC}$ values and the $UARL_{SIM}$ values since the maximum difference is close to 3%. In terms of the percent- age difference between the *AEQL* values computed using the Markov chain approach and simulations, it can be seen that the results of the two approaches are quite similar since the maximum percentage difference is less than 0.1%.

Table 9. The absolute percentage difference between the $UARL_{ZS}$ values computed using Markov chain and the $UARL_{ZS}$ values computed using simulations when (m, n) = (100, 5), h=1, 2 and 5 with a nominal ARL_0 value of 500 under the N(0,1), t(5) and GAM(1,1) distributions.

	DR scheme									KL scheme								
	N(0,1)			*t*(5)			*GAM*(1,1)			*N*(0,1)			*t*(5)			*GAM*(1,1)		
Shift	*h* = 1	*h* = 2	*h* = 5	*h* = 1	*h* = 2	*h* = 5	*h* = 1	*h* = 2	*h* = 5	*h* = 1	*h* =2	*h* = 5	*h* = 1	*h* = 2	*h* =5	*h* = 1	*h* =2	*h* =5
0.0	0.62	1.14	**1.43**	0.65	**1.71**	2.52	0.86	1.54	2.91	0.43	0.89	1.35	0.20	0.99	1.35	1.20	0.81	1.97
0.1	0.08	0.87	0.60	1.36	0.93	**2.65**	**2.36**	**3.04**	2.94	0.00	**1.21**	0.83	0.97	1.58	1.38	**2.76**	**2.98**	**3.01**
0.2	0.25	0.76	0.98	**1.60**	1.06	2.18	2.13	2.31	**3.12**	0.01	0.94	0.72	1.26	1.29	2.62	2.48	2.01	2.09
0.3	0.08	0.63	0.68	1.53	0.81	1.65	1.78	1.73	1.82	0.54	0.58	0.42	1.05	1.76	1.85	2.49	1.78	1.99
0.4	**0.63**	0.88	1.06	1.54	0.55	1.95	1.55	1.34	1.60	0.38	0.12	0.68	1.50	1.19	2.02	2.22	2.23	1.65
0.5	0.53	1.10	1.18	1.31	0.84	2.17	1.33	1.55	2.26	0.30	0.07	0.27	1.37	**1.94**	1.08	2.42	2.15	2.33
0.6	0.14	1.17	1.14	1.21	0.62	2.39	1.42	1.67	1.70	**0.67**	0.37	0.60	1.81	1.75	1.19	1.29	2.23	1.92
0.7	0.30	**1.18**	1.25	1.59	0.75	0.90	1.21	1.01	1.13	0.20	0.43	0.03	1.45	1.59	2.68	1.89	1.11	2.13
0.8	0.59	1.03	1.07	1.19	0.71	0.96	1.09	1.33	1.13	0.28	0.08	0.17	1.27	1.03	2.62	2.51	1.94	1.66
0.9	0.43	0.89	0.98	1.20	0.91	0.81	1.03	0.98	1.29	0.62	0.57	0.97	0.74	1.52	1.51	1.74	2.56	1.38
1.0	0.35	1.03	0.86	1.21	0.72	0.71	1.35	0.85	1.03	0.49	0.37	1.16	0.88	0.75	0.95	1.21	2.20	1.25
1.1	0.14	1.02	0.81	1.07	0.48	0.70	1.28	0.80	1.04	0.64	0.09	1.10	0.99	0.36	2.02	1.71	1.41	1.29
1.2	0.22	1.00	0.78	1.10	0.51	0.74	1.15	1.06	1.11	0.49	0.32	1.36	**1.89**	1.20	1.87	1.22	1.79	1.20
1.3	0.26	1.02	0.27	1.14	0.66	0.63	0.88	0.82	1.03	0.03	0.11	1.40	1.81	1.16	**2.81**	2.26	1.07	1.52
1.4	0.18	0.54	0.91	0.94	0.28	0.69	0.73	0.76	1.12	0.26	0.28	**1.44**	1.67	1.45	2.54	1.24	0.89	0.95
1.5	0.23	0.32	0.89	0.84	0.39	0.73	0.81	0.75	0.91	0.11	0.37	1.17	1.52	0.99	2.01	1.18	0.93	0.78
1.6	0.01	0.71	0.51	1.05	0.48	0.42	0.69	0.72	1.04	0.38	0.02	0.87	0.78	1.01	1.56	0.80	1.06	1.01
1.7	0.06	0.13	0.72	0.89	0.35	0.46	0.70	0.42	1.08	0.27	0.08	0.47	0.95	0.59	0.85	0.74	0.66	0.36
1.8	0.29	0.23	0.63	0.83	0.04	0.29	0.73	0.30	1.05	0.01	0.01	0.52	0.48	0.55	0.78	0.63	1.08	0.33
1.9	0.05	0.40	0.75	0.71	0.22	0.21	0.69	0.58	1.05	0.13	0.22	0.14	0.60	0.64	0.66	0.39	1.03	0.53
2.0	0.18	0.38	0.71	0.24	0.27	0.13	0.51	0.49	0.43	0.17	0.01	0.10	0.03	0.49	0.20	0.30	0.90	0.18
2.5	0.12	0.12	0.28	0.05	0.05	0.08	0.42	0.40	0.04	0.09	0.08	0.18	0.04	0.04	0.06	0.30	0.60	0.32
3.0	0.03	0.03	0.06	0.00	0.00	0.01	0.08	0.22	0.21	0.02	0.02	0.04	0.00	0.00	0.00	0.04	0.22	0.19
AEQL	0.02	0.03	0.04	0.01	0.03	0.05	0.03	0.04	0.06	0.01	0.03	0.04	0.02	0.03	0.05	0.02	0.04	0.07

5.2 Effect of the Phase I sample size on the performance of the proposed schemes

In real-life applications and specifically in manufacturing processes, the underlying quality process distribution is mostly non-normal with unknown parameters (Case U). In this case, the IC process parameters need to be estimated before process monitoring can begin. Using parameter estimates degrades charts performances and may also give more false alarms than expected. Many researchers pointed out the deterioration of the Phase II scheme performance due to the effect of estimation error (Bischak and Trietsch, 2007; Castagliola et al., 2012). In such a case, a study of the effects (or impact) of parameter estimation on the control chart performance is recommended and it focuses mostly on the IC characteristics of the run-length distribution (Saleh et al., 2015). While studying the effects of parameter estimation on the Phase II chart performance, it is useful to examine the conditional run-length (CRL) distribution. The CRL distribution and various associated issues have been studied by several authors, including Chakraborti (2006) for Shewhart-type schemes. In this section, we focus on the impact (or effect) of the Phase I reference sample size on the performance of the proposed precedence schemes with respect to the CRL distribution and its characteristics such as the conditional IC average run-length ($CARL_0$) and conditional IC standard deviation of run-length ($CSDRL_0$).

The number of observations available for a Phase I analysis plays a crucial role in the estimation of the values of any unknown parameters. Jensen et al. (2006) studied the effect of estimation error on control charts performances in Phase II. They concluded that the accurate and precise estimation of any unknown process parameters is critical for achieving a specified Phase II chart performance and the size of the Phase I sample must often be quite large in order to achieve the accurate and precise estimation needed. In order to answer the question of the size of the Phase I sample needed for the enhanced precedence schemes, we make use of the mean of the conditional $ARL_0 (CAARL_0)$ and the conditional standard deviation of the ARL_0 $(CSDARL_0)$. The size of the Phase I reference sample is estimated such that the $CAARL_0$ is close to the desired value of 500 and the $CSDARL_0$ values within 10% of the intended ARL_0 as recommended by Zhang et al. (2014).

The Monte Carlo simulation steps in the Phase I sample size study of the proposed precedence schemes are given as follows:

Step 1: For each Phase I sample size (say m = 100), we compute the $M \times M$ IC CRL (CRL_0) matrix $CRL_{0_{M \times M}}$ where M is the number of simulations (or replications).

Step 2: Compute the $CARL_0$ vector, $CARL_{0_{M\times 1}}$, and the associated IC conditional standard deviation of the run-length ($CSDRL_0$) vector, $CSDRL_{0_{M \times 1}}$.

Step 3: Compute the $CARL_0$ and $CSDRL_0$ u - quantiles (they are equivalent to the percentiles; for instance, u = 0.10 represents the 10th percentile, u = 0.11 represents the 11th percentile,…, u = 0.9 represents the 90th percentile etc.). This step allows us to estimate the position (in percentage of the sample size) that guarantee the best estimate of the plotting constant (see Figure 3).

Step 4: Repeat Steps 1 to 3 for the different Phase I sample size, m.

Step 5: For each triplet (m, a, b), compute the mean of the $CARL_0$ vector ($CAARL_0$) and the standard deviation of the $CARL_0$ vector ($CSDARL_0$) for different value of m. Record the $CAARL_0$ and $CSDARL_0$ values next to their corresponding triplet (m, a, b).

Step 6: Select the Phase I sample size such that the $CAARL_0$ value is close to the nominal ARL_0 and the $CSDARL_0$ value within the 10% of the nominal ARL_0. This sample size represents the number of Phase I observations needed in order to achieve a stability and better Phase II performance of the proposed schemes.

Note that the design of the proposed schemes requires the estimation of the plotting constants a and b. Once one plotting constant is found, the other may be easily determined through the expression defining the relationship between a, b and m; that is, $a + b = m + 1$ which means $a = m - b + 1$. From Figures 3 (a)-(c) it can be seen that, for the DR scheme, the proposed scheme performs better if the estimate of the plotting constant b is near the 70th percentile when m = 500 and h = 1. For $100 \leq m < 500$, the proposed scheme performs better when b is between the 85th and 95th percentiles. When h = 2, the proposed scheme performs better when b is between the 75th and 95th percentiles and $m \in$ {25, 50, 100, 200, 300, 400} and near the 50th percentile when m = 500. When h = 5, the proposed scheme performs better when b is between the 40th and 50th percentiles and $m \in$ {200, 300, 400} and between the 80th and 95th percentiles when m = 100 and 500. From Figures 3 (d)-(f), for the KL scheme, it can be seen that the proposed 2-*of*-2 (i.e., h = 1) scheme performs better when the estimate of the plotting constant b is near the 70th and 90th percentiles and $m \in$ {400, 500} and {100, 200, 400}, respectively. For more details on the position of the estimate of the plotting constants, the reader is referred to Figure 3 at the intersection of each $CARL_0$ curve and $CARL_0$ = 500 (the position is read on x −axis).

Table 10 displays the $CAARL_0$ and its corresponding $CSDRL_0$ values in brackets for different (m, a, b) triplets of the Shewhart 2-*of*-(*h*+1) precedence schemes. The results clearly illustrate the potential problems associated with parameter estimation. The shaded cells of Table 9 give the number of Phase I observations that guarantee stability and better performance of the proposed schemes. It can be seen that, the Shewhart 2-*of*-2 and 2-*of*-3 DR precedence schemes require at least 200 Phase I observations, while the 2-*of*-6 DR precedence scheme requires at least 300 Phase I observations. The 2-*of*-2 and 2-*of*-6 KL precedence schemes require at least 200 Phase I observations, while the 2-*of*-6 KL precedence scheme requires at least 100 Phase I observations.

Table 10. The $CAARL_0$ and $CSDEL_0$ (in brackets) of the Shewhart 2-*of*-(*h*+1) DR and KL precedence schemes when h = 1, 2 and 5 for a nominal ARL_0 of 500

		DR			KL		
	h	1	2	5	1	2	5
m	25	269.73 (21.96)	183.65 (75.07)	74.65 (8.55)	136.7 (30.09)	310.00 (90.23)	126.54 (20.82)
	50	283.84 (21.64)	315.74 (46.88)	359.44 (75.53)	461.17 (60.32)	521.41 (78.00)	433.53 (52.12)
	100	536.03 (24.36)	437.23 (30.30)	481.42 (40.09)	457.43 (25.91)	494.90 (33.88)	542.83 (44.90)
	200	524.42 (20.60)	527.27 (25.86)	466.73 (26.74)	471.79 (20.53)	503.10 (22.8)	502.56 (29.64)
	300	471.69 (17.68)	487.85 (20.16)	480.68 (26.56)	479.77 (18.73)	512.32 (21.29)	503.86 (31.87)
	400	477.35 (15.95)	524.12 (20.53)	510.83 (26.20)	487.33 (18.88)	518.89 (19.67)	511.16 (30.09)
	500	492.59 (16.71)	500.64 (18.61)	506.39 (19.48)	489.56 (17.82)	488.37 (17.05)	471.33 (17.75)

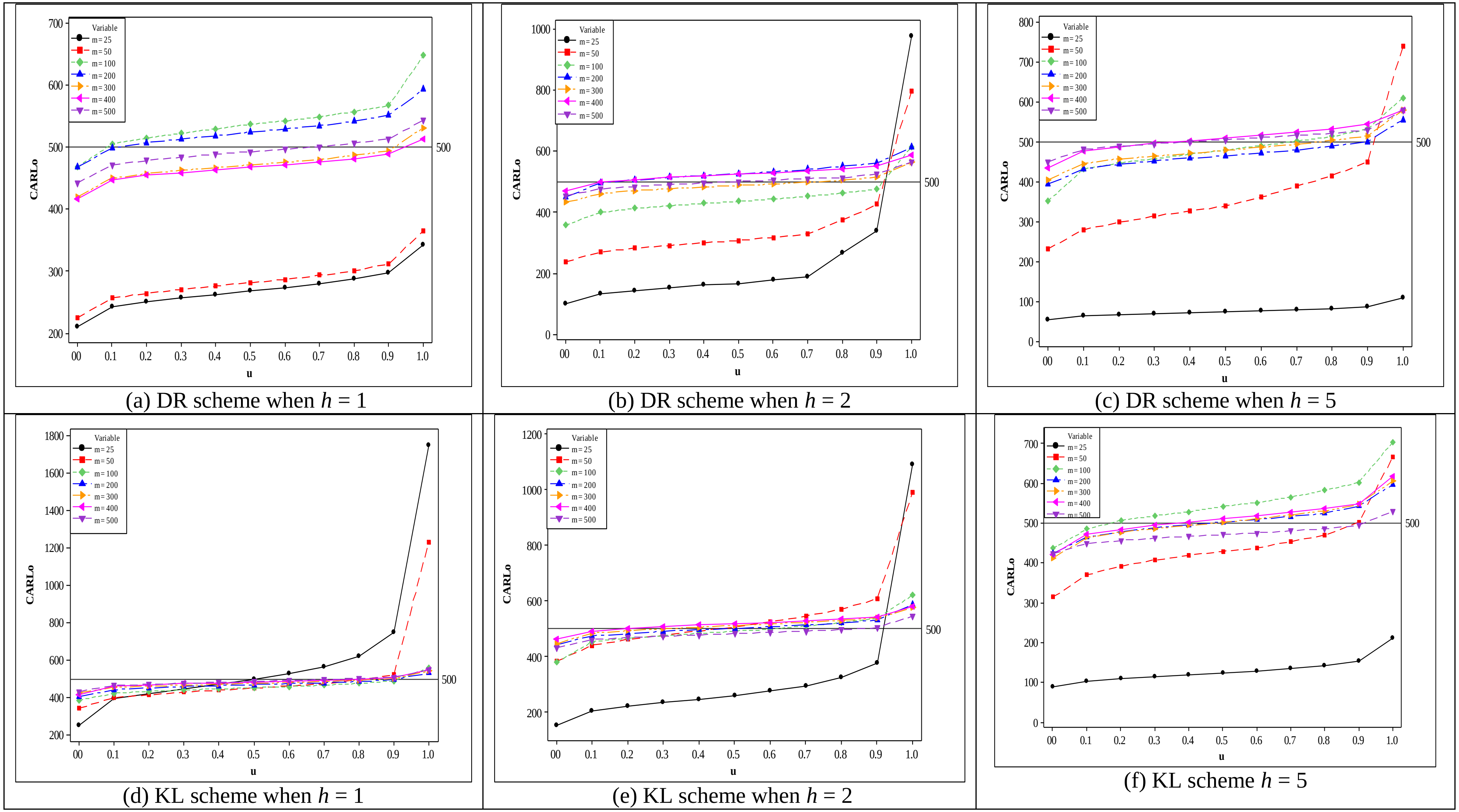

(a) DR scheme when h = 1

(b) DR scheme when h = 2

(c) DR scheme when h = 5

(d) KL scheme when h = 1

(e) KL scheme when h = 2

(f) KL scheme h = 5

Figure 3. The $CARL_0$ of the 2-of-(h+1) precedence schemes for different values of the triplet (m, a, b) and u quantiles, when n = 5 and h = 1, 2 and 5

6. Illustrative example

In this section, we illustrate the design and implementation of the proposed schemes using a well-known dataset from Montgomery (2001, page 223, Tables 5.2 and 5.3). The data are the inside diameters of piston rings manufactured by a forging process. The data given in Table 5.2 contains fifteen Phase II samples, each of size n = 5. Table 5.3 contains 125 Phase I observations, that were collected when the process was considered IC (m = 125). These data are considered to be the Phase I (or reference) observations for which a goodness of fit test for normality is not rejected.

For both zero-state and steady-state modes, for a nominal $ZSARL_0$ (or $SSARL_0$) of 500, the zero-state and steady-state LCL and UCL of the 2-*of*-(h+1) DR precedence schemes with h = 1 (i.e., 2-*of*-2 scheme) are given by LCL_1 = $X_{(19:125)}$ = 73.99 and UCL_1 = $X_{(107:125)}$ = 74.012, respectively. The subscript 1 from the LCL and UCL refers to the value of h. The zero-state and steady-state LCL and UCL of the 2-*of*-4 DR precedence scheme are given by LCL_3 = $X_{(16:125)}$ = 73.99 and UCL_3 = $X_{(110:125)}$ = 74.013, respectively. A plot of the median plotting statistics for both cases is shown in Figure 4 (a). It is seen that 2-*of*-2 DR precedence scheme signals for the first time on the tenth sample in the prospective phase (Phase II), whereas the 2-*of*-4 DR precedence scheme signals for the first time on the twelfth sample in the prospective phase.

The zero-state and steady-state LCL and UCL of the 2-*of*-2 and 2-*of*-4 KL precedence scheme are given by (LCL_1, UCL_1) = ($X_{(21:125)}$, $X_{(105:125)}$) = (73.992, 74.011) and (LCL_3, UCL_3) = ($X_{(17:125)}$, $X_{(119:125)}$) = (73.986, 74.013), respectively. A plot of the median plotting statistics for both cases is shown in Figure 4 (b). It is seen that 2-*of*-2 KL precedence scheme signals for the first time on the tenth sample in the prospective phase (Phase II), whereas the 2-*of*-4 KL precedence scheme signals for the first time on the twelfth sample in the prospective phase.

The example shows that the 2-*of*-2 DR and KL schemes outperform the 2-*of*-4 DR and KL schemes. This agrees with our finds in Section 4.3.

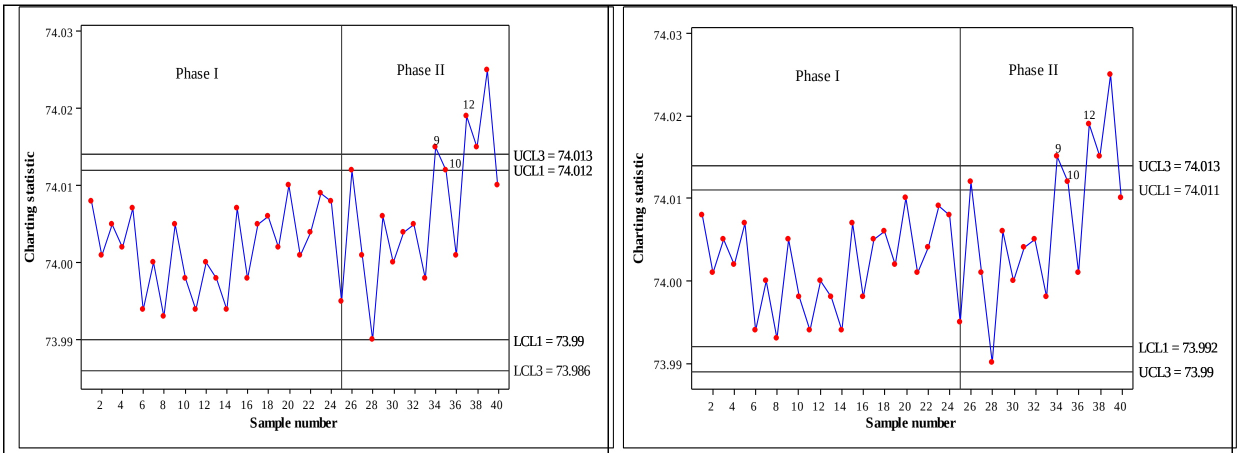

(a) ZS and SS DR scheme of the 2-*of*-(h+1) precedence schemes when m = 125, n = 5 with h = 1 and 3	(b) ZS and SS KL scheme of the 2-*of*-(h+1) precedence schemes when m = 125, n = 5 with h = 1 and 3

Figure 4. The 2-*of*-2 and 2-*of*-4 DR and KL precedence schemes for the Montgomery (2001) piston ring data

7. Summary and conclusion

Chakraborti et al. (2004) proposed a class of nonparametric Shewhart-type schemes, called the precedence scheme, using some order statistic of a Phase II sample as the charting statistic and control limits constructed using some order statistics of the Phase I reference sample. Chakraborti et al. (2009) improved the precedence scheme by using the 2-*of*-2 DR and KL runs-rules using a backward Markov chain approach. Malela-Majika et al. (2016b) proposed the 2-*of*-2 KL minimum and median precedence schemes using simulations. In this paper, we proposed the generalized 2-*of*-(h+1) DR and KL precedence schemes using a forward Markov chain approach. The performance of the proposed charts is thoroughly investigated in order to suggest the most efficient precedence monitoring scheme.

Chakraborti et al. (2009) showed that the 2-*of*-2 DR and KL schemes enhance the basic precedence schemes. In this paper, we showed that the addition of runs-rules to the basic precedence scheme does not always improve its performance in some of the cases. Therefore, a thorough investigation of the performance of control schemes supplemented with different types of runs-rules is needed. The performance analysis confirms that proposed 2-*of*-(h+1) KL precedence schemes perform better than the 2-*of*-(h+1) DR precedence schemes.

The performance analysis showed that there is not a specific value of h that provides a superior precedence scheme. Therefore, quality practitioners are recommended to use the value of h between 2 and 6 ($2 \leq h \leq 6$) in order to monitor efficiently small and moderate shifts. In case practitioners are interested to monitor processes where δ_{max} = 3 using the precedence scheme with supplementary 2-*of*-(*h*+1) runs-rules, they would be advised to use *h* = 4 or 5. In practice, we would recommend operators and quality practitioners to make use of small values of h for two main reasons: (i) simplicity in the design and implementation of schemes, (ii) higher efficiency in monitoring small and moderate shifts.

In future, we will consider investigating the performance of the improved 2-*of*-(*h*+1), modified 2-*of*-(*h*+1), improved modified 2-*of*-(*h*+1), *h*-*of*-*h* (with *h* = 2, 3, …), improved *h*-*of*-*h* and the synthetic precedence control charts. Also, in this paper we only considered symmetric control limits and the proposed schemes, using non-symmetric control limits, will be investigated as a future research problem.

Acknowledgements

The authors thank Mr. Sandile Shongwe from the University of Pretoria for his helpful comments and suggestions. They also thank the University of South Africa for the support.

References

Albers, W. and W. C. M. Kallenberg. 2008a. Minimum control charts. *Journal of Statistical Planning and Inference* 138 (3):539-51.

Albers, W. and W. C. M. Kallenberg. 2008b. MINDCUMIN charts. *Journal of Nonparametric Statistics* 20 (8):769-90.

Balakrishnan, N., and M.V. Koutras. 2002. *Runs and scans with applications*. John Wiley & Sons: New York.

Balakrishnan, N., Paroissin, C., and J.-C. Turlot. 2015. One-sided control charts based on Precedence and Weighted Precedence Statistics. *Quality and Reliability Engineering International* 31: 113-134.

Bischak, D.P., and D. Trietsch. 2007. The rate of false signals in $\overline{X}$ charts with estimated limits. *Journal of Quality Technology* 39(1): 54 – 65.

Castagliola, P., Zhang, Y., Costa, A., and P. Maravelakis. 2012. The variable sample size $\overline{X}$ chart with estimated parameters. *Quality and Reliability Engineering International* 28(7): 687- 699.

Chakraborti, S. 2006. Parameter estimation and design considerations in prospective applications of $\bar{X}$- chart. *Journal of Applied Statistics* 33(4): 439-459.

Chakraborti, S., Eryilmaz, S., and S.W. Human. 2009. A phase II nonparametric control chart based on precedence statistics with runs-type signaling rules. *Computational Statistics and Data Analysis* 53(4): 1054-1065.

Chakraborti, S., Van der Laan, P., and M.A. Van de Wiel. 2004. A class of distribution-free control charts. *Journal of the Royal Statistical Society. Series C: Applied Statistics* 53(3): 443-462.

Chang, H. M., Chang, Y. M., Fu, W. H., and W.C. Lee. 2018. On limiting theorems for conditional causation probabilities of multiple-run-rules. *Statistics & Probability Letters*. DOI: 10.1016/ j.spl.2018.02.069.

Derman, C., and S.M. Ross. 1997. *Statistical aspects of quality control*. Academic Press: San Diego.

Dyer, J.N. 2016. Monte Carlo simulation design for evaluating normal-based control chart properties. *Journal of Modern Applied Statistical Methods* 15(2): 580-626.

Graham, M.A., Mukherjee A., and S. Chakraborti. 2017. Design and implementation issues for a class of distribution-free Phase II EWMA exceedance control charts. *International Journal of Production Research* 55(8): 2397-2430.

Golbafian, V., Fallahnezhad, M. S., and Y. Zare Mehrjerdi. 2017. A new economic scheme for CCC charts with Run Rules based on Average Number of Inspected Items. *Communications in Statistics-Theory and Methods* 46(24): 12023-12044.

Human, S.W., Chakraborti, S., and C.F. Smit. 2010. Nonparametric Shewhart-type sign control charts based on runs. *Communications in Statistics: Theory and Methods* 39(11): 2046 – 2062.

Janacek, G.J., and S.E. Meikle. 1997. Control charts based on medians. *The Statistician* 46(1): 19-31.

Jensen, W.A., Jones-Farmer, L.A., Champ, C.W., and W.H. Woodall. 2006. Effects of parameter estimation on control chart properties: A literature review. *Journal of Quality Technology* 38(4): 349-364.

Klein, M. 2000. Two alternatives to Shewhart $\bar{X}$ control chart. *Journal of Quality Technology* 32: 427-431.

Kritzinger, P., Human, S.W., and S. Chakraborti. 2014. Improved Shewhart-type runs-rules nonparametric sign charts. *Communications in Statistics – Theory and Methods* 43(22): 4723-4748.

Lee, M. H., and M.B. Khoo. 2017. Economic-statistical design of control chart with runs rules for correlation within sample. *Communications in Statistics-Simulation and Computation* 1-16. DOI:10.1080/03610918.2017.1361977.

Li C, Mukherjee A, Su Q, and M. Xi. 2016. Robust algorithms for economic designing of a nonparametric control chart for abrupt shift in location. *Journal of Statistical computation and Simulation* 86(2): 306-323.

Li Z, Zou C, Gong Z, and Z. Wang. 2014. The computation of average run length and average time to signal: an overview. *Journal of Statistical computation and Simulation* 84(8): 1779-1802.

Machado, M.A.G., and A.F.B. Costa. 2014. A side-sensitive synthetic chart combined with an $\bar{X}$ chart. *International Journal of Production Research* 52(11): 3404-3416.

Malela-Majika, J.C., Chakraborti, S., and M.A. Graham. 2016a. Distribution-free Phase II Mann-Whitney control charts with runs-rules. *International Journal of Advanced Manufacturing Technology* 86: 723-735.

Malela-Majika, J.C., Chakraborti, S., and M.A. Graham. 2016b. Distribution-free precedence control charts with improved runs-rules. *Applied Stochastic Models in Business and Industry* 32: 423-439.

Maravelakis, P. E., Castagliola, P., and M.B. Khoo. 2017. Run length properties of run rules EWMA chart using integral equations. *Quality Technology & Quantitative Management*, DOI: 10.1080/16843703.2017.1372853.

Mehmood, R., Qazi, M.S., and M. Riaz. 2018. On the performance of $\bar{X}$ control chart for known and unknown parameters supplemented with runs-rules under different probability distributions. *Journal of Statistical computation and Simulation* 88(4): 675-711.

Montgomery, D.C. 2001. *Introduction to Statistical Quality Control* (4th ed.). New York: Wiley.

Montgomery, D.C. 2013. *Introduction to Statistical Quality Control* (7th ed.). John Wiley, New York, NY.

Mukherjee, A., and R. Sen. 2018. Optimal design of Shewhart-Lepage type schemes and its application in monitoring service quality. *European Journal of Operational Research* 266(1): 147-167.

Nelson, L.S. 1984. Shewhart control chart-tests for special cases. *Journal of Quality*

Technology 16(4): 237-239.

Patil SH, and D.T. Shirke. 2017. Economic design of nonparametric sign control chart. *Communications in Statistics-Theory and Methods* 46(18): 8987-8998.

Petcharat, K., Sukparungsee, S., and Y. Areepong. 2015. Exact solution of the average run length for cumulative sum chart for a moving average process of order q. *Science Asia*, 41: 141-147.

Qiu, P. 2014. *Introduction to Statistical Process Control*. CRC Press, Taylor & Francis Group, A Chapman & Hall Book, Boca Raton, Florida.

Rakitzis, AC. 2016. Monitoring exponential data using two-sided control chart with runs-rules. *Journal of Statistical computation and Simulation* 86(1): 149-159.

Rakitzis, A. C. 2017. On the performance of modified runs rules charts with estimated parameters. *Communications in Statistics-Simulation and Computation* 46(2): 1360-1380.

Reynolds, M.R. Jr., and L. Lou. 2010. An evaluation of GLR control chart combined with an $\bar{X}$ chart. *Journal of Quality Technology* 42(3): 287-310.

Saleh, N.A., Mahmoud, M.A., Keefe, M.J., and W.H. Woodall. 2015. The difficulty in designing Shewhart X-bar and X control charts with estimated parameters. *Journal of Quality Technology* 47(2): 127-138.

Shongwe, S.C., and M.A. Graham. 2016. On the performance of Shewhart-type synthetic and runs-rules charts combined with an $\bar{X}$ chart. *Quality and Reliability Engineering International* 32(4): 1357-1379.

Tran, K. P. 2017. Run Rules median control charts for monitoring process mean in manufacturing. *Quality and Reliability Engineering International* 33(8): 2437-2450.

Tran, K.P. 2018. Designing of run rules t charts for monitoring changes in the process mean. *Chemometrics and Intelligent Laboratory System* 174: 84-93.

Triantafyllou, I.S. 2017. Nonparametric control charts based on order statistic: Some advances. *Communications in Statistics- Simulation and Computation* DOI: 10.1080/03610918.2017. 1359283.

Trip, A., and R.J.M.M. Does. 2010. Quality Quandaries: Interpretation of signals from runs rules in Shewhart control charts. *Quality Engineering*, 22: 351-357.

Western Electric Company. 1956. *Statistical Quality Control Handbook*. Western Electric Company: Indianapolis, IN.

Wu, Z., and M.B.C. Khoo. 2008. Optimisation designs of the combined Shewhart-CUSUM control charts. *Computational Statistics and Data Analysis* 53(2): 496-506.

Zhang, M., Megahed, F.M., and W.H. Woodall. 2014. Exponential CUSUM charts with estimated control limits. *Quality and Reliability Engineering International* 30: 275-286.

Zombade DM, and V.B. Ghute. 2018. Shewhart-type nonparametric control chart for process location. *Communications in Statistics-Theory and Methods* DOI10.1080/03610926.2018.1435811.